Geochemistry - Interdisciplinary Journal for Chemical Problems of the Geosciences and Geoecology xxx (xxxx) xxx

Contents lists available at ScienceDirect

Geochemistry

journal homepage: www.elsevier.com/locate/chemer

Earth and Mars – Distinct inner solar system products

Takashi Yoshizaki [a,*], William F. McDonough [a,b,c]

[a] Department of Earth Science, Graduate School of Science, Tohoku University, Sendai, Miyagi 980-8578, Japan
[b] Department of Geology, University of Maryland, College Park, MD 20742, USA
[c] Research Center for Neutrino Science, Tohoku University, Sendai, Miyagi 980-8578, Japan

ARTICLE INFO

Handling Editor: Carita Augustsson

Keywords:
Earth
Mars
Chondrites
Solar system
Cosmochemistry

ABSTRACT

Composition of terrestrial planets records planetary accretion, core–mantle and crust–mantle differentiation, and surface processes. Here we compare the compositional models of Earth and Mars to reveal their characteristics and formation processes. Earth and Mars are equally enriched in refractory elements (1.9 × CI), although Earth is more volatile-depleted and less oxidized than Mars. Their chemical compositions were established by nebular fractionation, with negligible contributions from post-accretionary losses of moderately volatile elements. The degree of planetary volatile element depletion might correlate with the abundances of chondrules in the accreted materials, planetary size, and their accretion timescale, which provides insights into composition and origin of Mercury, Venus, the Moon-forming giant impactor, and the proto-Earth. During its formation before and after the nebular disk's lifetime, the Earth likely accreted more chondrules and less matrix-like materials than Mars and chondritic asteroids, establishing its marked volatile depletion. A giant impact of an oxidized, differentiated Mars-like (i.e., composition and mass) body into a volatile-depleted, reduced proto-Earth produced a Moon-forming debris ring with mostly a proto-Earth's mantle composition. Chalcophile and some siderophile elements in the silicate Earth added by the Mars-like impactor were extracted into the core by a sulfide melt (~0.5% of the mass of the Earth's mantle). In contrast, the composition of Mars indicates its rapid accretion of lesser amounts of chondrules under nearly uniform oxidizing conditions. Mars' rapid cooling and early loss of its dynamo likely led to the absence of plate tectonics and surface water, and the present-day low surface heat flux. These similarities and differences between the Earth and Mars made the former habitable and the other inhospitable to uninhabitable.

1. Introduction

Earth and Mars share many chemical and physical attributes, but are distinct in size and inventory of volatile elements. Chemical data from surface rocks and meteorites combined with seismological and geodetic observations (e.g., mass, density, moment of inertia (MOI)) provide a multiply constrained compositional model of the terrestrial planets (e.g., Ringwood, 1966; Morgan and Anders, 1980; Wänke, 1981; Longhi et al., 1992). The physicochemical similarities and differences between Earth and Mars provide useful insights on formation and evolution processes of these bodies, and potentially provide insights into the present-day properties and origin of other rocky bodies (Venus, Mercury, and exoplanets).

By definition, Earth and Mars are located within a habitable zone in which liquid water is available (Cockell et al., 2016; Ehlmann et al., 2016). However, currently life exists only on Earth, and it remains unclear if Mars were inhabited or uninhabited in its history. The occurrence of life only on Earth indicates that there are compositional limits for a habitable planet formation, which can be revealed by an Earth-Mars comparison. Previous comparative studies of chemical compositions of the interiors of Earth and Mars described their differences including abundances of volatile or siderophile elements and redox states (Anders and Owen, 1977; Dreibus and Wänke, 1987; Wänke and Dreibus, 1994), but the recent advances in compositional modeling of both Earth and Mars will provide further insights into their characters and origins.

Isotopic compositions of solar system materials provide strong constraints on the sources of the terrestrial planets. Mass-independent, nucleosynthetic isotope anomalies in meteorites reveal a heterogeneous distribution of distinct presolar materials and provide the basis for classifying the non-carbonaceous (NC) and carbonaceous meteorite (CC) groups (Trinquier et al., 2007, 2009; Warren, 2011; Kruijer et al.,

* Corresponding author.
E-mail address: takashiy@tohoku.ac.jp (T. Yoshizaki).

https://doi.org/10.1016/j.chemer.2021.125746
Received 12 October 2020; Received in revised form 27 January 2021; Accepted 1 February 2021
Available online 10 February 2021

Please cite this article as: Takashi Yoshizaki, William F. McDonough, *Geochemistry - Interdisciplinary Journal for Chemical Problems of the Geosciences and Geoecology*, https://doi.org/10.1016/j.chemer.2021.125746

2017a). The NC meteorites appear to be from the inner solar system, whereas the CC meteorites are considered to be samples from the outer solar system, including the Trojan asteroids and possibly beyond Jupiter's orbit (Walsh et al., 2011; Kruijer et al., 2017a). These isotopic observations demonstrate a link between Earth and enstatite chondrites, whereas Mars is thought to be most closely related to ordinary chondrites (e.g., Trinquier et al., 2007, 2009; Javoy et al., 2010; Warren, 2011; Dauphas, 2017).

Here we compare the compositional models of Earth (e.g., McDonough et al., 1995; Palme and O'Neill, 2014) and Mars (e.g., Wänke and Dreibus, 1994; Taylor, 2013; Yoshizaki and McDonough, 2020) to clarify their characteristics and formation processes. We explore the nature of the building blocks of the terrestrial planets, based on their compositional similarities and differences with chondritic meteorites. These comparisons provide a basis for insights into the conditions for habitable planet formation and evolution.

2. Comparisons

2.1. Bulk planet

The geochemical classification of elements consists of four element groups: lithophile (rock-loving), siderophile (metal-loving), chalcophile (sulfide-loving), and atmophile elements. Lithophile elements (e.g., Si, Mg, Ca, Al, Ti, Na, K, rare earth elements) are preferentially incorporated into oxide phases, and thus concentrated in a silicate shell in a differentiated planetary body. Therefore, their abundances in the mantle can be converted to the bulk composition if we also know a mass fraction of a metallic core in a planet. In addition, elements are also classified based on their volatilities in a gas of solar composition at 10 Pa (Lodders, 2003).

Historically, there have been three families of compositional models for the bulk silicate Earth, in terms of the proportions of the refractory elements relative to Mg and Si, which, together with Fe and O, make up ~90% of rocky planets. These models have low (Javoy, 1995; Javoy et al., 2010; Warren, 2008; Caro and Bourdon, 2010), medium (Ringwood, 1975; Jagoutz et al., 1979; Wänke, 1981; Hart and Zindler, 1986; Allégre et al., 1995; McDonough et al., 1995; Palme and O'Neill, 2014), and high (Wasserburg et al., 1963; Turcotte et al., 2001; Turcotte and Schubert, 2014) proportion of refractory elements (McDonough, 2016 and references therein). Here we estimate a primitive (i.e., the least melt-depleted) mantle composition based on compositional trends from basalts and mantle rocks and propose a model with medium refractory element abundance (e.g., McDonough et al., 1995; Palme and O'Neill, 2014; see also Section A.1). As summarized in Palme and O'Neill (2014), these geochemical models of Earth are basically similar to each other, and differences between the models do not affect comparison of Earth and Mars discussed in the current paper.

A similar geochemical approach has been applied in constraining compositional models of Mars (Wänke and Dreibus, 1994; Taylor, 2013; Yoshizaki and McDonough, 2020). Here we adopt the compositional model by Yoshizaki and McDonough (2020), which is compositionally and mineralogically similar to those of Wänke and Dreibus (1994) and Taylor (2013) (Fig. A.1; see also Bertka and Fei, 1997; Khan et al., 2018; Smrekar et al., 2019 for Martian mantle mineralogy models), but differ in model development. For example, Wänke and Dreibus (1994) assumed that Mn and more refractory elements (including Fe, Mg and Si) are in chondritic relative abundances in bulk Mars, which is denied by Yoshizaki and McDonough (2020). The details of previous Mars models are summarized by Taylor (2013) and Yoshizaki and McDonough (2020).

By establishing the planet's budget of the 36 refractory elements, recognizing that ratios of refractory elements (e.g., Ca/Al, Th/U) and Fe/Ni are constant (±15% or better) in the chondritic building blocks (e.g., Wasson and Kallemeyn, 1988; Alexander, 2019a,b), and either knowing the relative mass of the planet's core or the mantle's Mg# (atomic ratio of Mg/(Mg + Fe)), limit the range of acceptable Mg/Si (i.e., olivine/pyroxene) values for planetary compositional models (Figs. 1 and 2 A). The Fe/Mg vs Fe/Si correlation seen in both the NC and CC chondrites is suggestive of metal-silicate gradients in the solar system (Figs. 1 and 2 B); interestingly, Earth and Mars also follow this correlation.

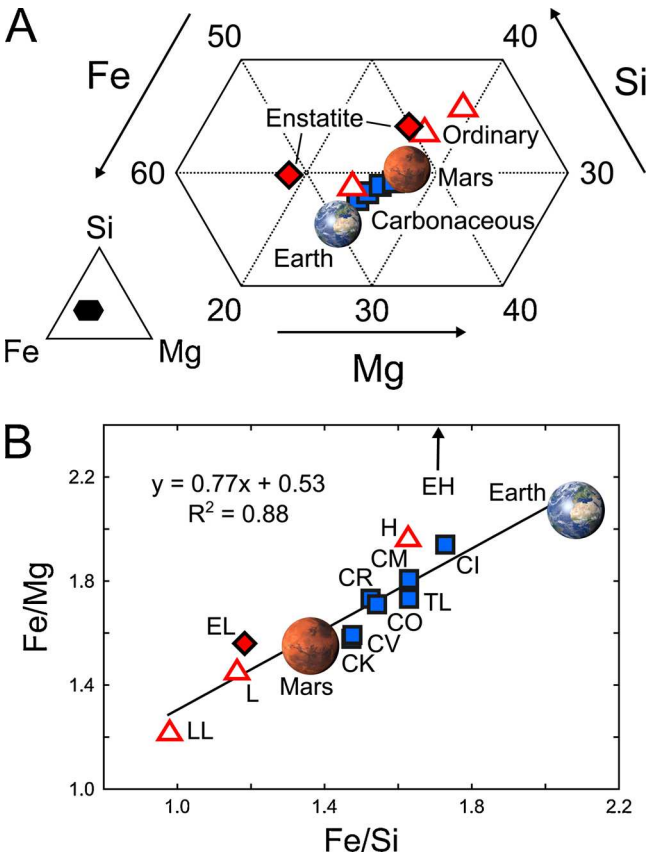

Fig. 1. (A) Ternary plot and (B) scatter ratio plot of major elements Si, Fe and Mg in bulk Earth (McDonough, 2014), bulk Mars (Yoshizaki and McDonough, 2020) and chondritic meteorites (Alexander, 2019a,b). The regression line for chondrites (except for sulfide-rich EH) is also shown in the lower panel. TL, Tagish Lake.

The approach used here finds that the bulk Earth contains 1.85 × CI abundances for the refractory elements (e.g., McDonough et al., 1995; Palme and O'Neill, 2014), it has an olivine/pyroxene proportion equivalent to that of pyrolite (Ringwood, 1966), and is depleted in volatile elements (i.e., sub-CI Rb/Sr, K/U, and S; Fig. 3A; Gast, 1960; Wasserburg et al., 1964). Mars also contains ~ 1.9 × CI abundances for the refractory elements and is depleted in volatile elements, but less so than Earth (Fig. 3B; Yoshizaki and McDonough, 2020). The net atomic oxygen/(metallic Fe) values of Earth and Mars (3.7 and 8.7, respectively; Table 1) provide a measure of its average oxidation state. These compositional models for Earth and Mars provide a time-integrated perspective for materials available for accretion at 1 and 1.5 AU, respectively. This spatial sampling contrasts with the temporal comparison, as the mean timescales for Mars' formation ($\tau_{\mathrm{Mars}}^{\mathrm{accretion}} \sim 2$ Myr; Dauphas and Pourmand, 2011) differs from that for Earth ($\tau_{\mathrm{Earth}}^{\mathrm{accretion}} \gtrsim 30$ Myr; Kleine et al., 2009).

2.2. Bulk silicate planet

2.2.1. Geochemistry and mineralogy

Chondritic ratios of refractory lithophile elements in the bulk silicate Earth and Mars (BSE and BSM, respectively) are further confirmed and

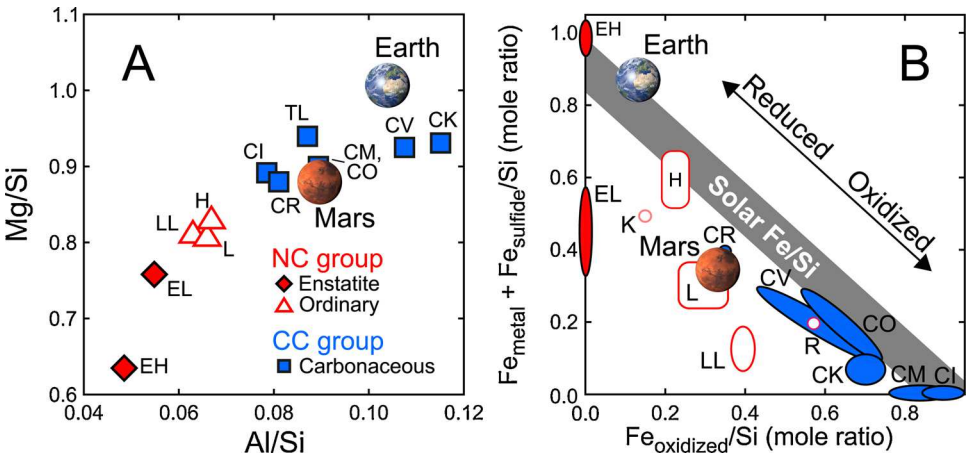

Fig. 2. (A) Weight ratios of Al/Si vs Mg/Si values for planets and chondrites. Earth and Mars show higher RLE abundances (i.e., Al) and Mg/Si value (i.e., olivine/pyroxene ratio) compared to enstatite and ordinary chondrites, which are respectively their isotopically identified relatives. (B) The Urey–Craig diagram (after Urey and Craig, 1953) illustrates relative redox condition for Earth, Mars, and chondrites. Chondrite classification (non-carbonaceous (NC; red) vs carbonaceous (CC; blue) groups) follows Warren (2011) and Kruijer et al. (2017a). TL, Tagish Lake. Data sources are as in Fig. 1.

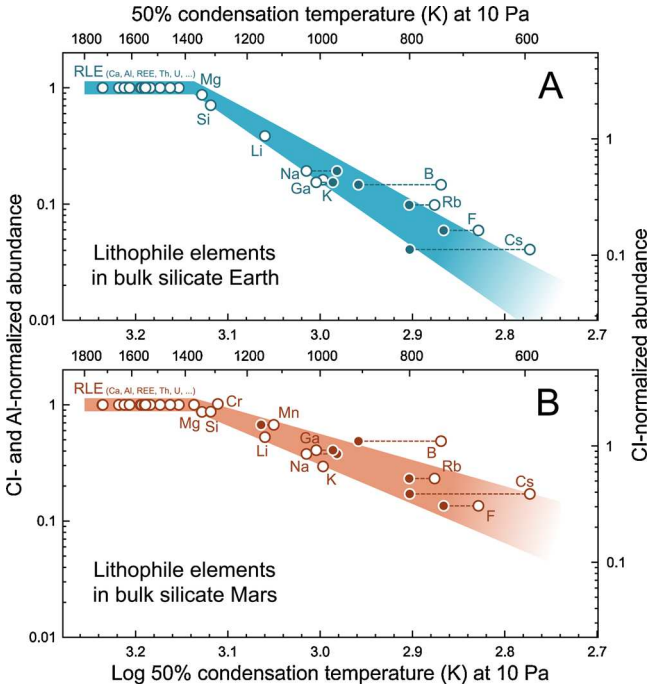

Fig. 3. Lithophile element abundances in the bulk silicate Earth and Mars normalized to CI abundances and refractory lithophile element Al. The scale of right ordinate shows the CI-normalized abundances. The values are plotted against 50% condensation temperature (K) of elements at 10 Pa (open; Wood et al., 2019) and (filled; Lodders, 2003). CI abundance is from Lodders (2020). Other data sources are as in Fig. 1.

constrained by Lu-Hf, Sm-Nd and La-Ce isotopic systematics of these planetary materials (e.g., Bouvier et al., 2008; Burkhardt et al., 2016; Willig et al., 2020). The moderately volatile, lithophile elements (lithophile MVE; e.g., alkali metals) are depleted in Earth and Mars when compared to chondritic meteorites, both planets showing comparable correlations with their condensation temperatures (Fig. 3). Earth, with K/U of 14,000 and Rb/Sr of 0.032 (i.e., MVE/refractory ratios; cf., 68,000 and 0.30 in CI chondrites, respectively), shows such a strong depletion trend in these elements (Fig. 3A). Mars, with a K/U of 20,000 and Rb/Sr of 0.068, also shows this trend (Fig. 3B), albeit less depleted than the Earth's.

Siderophile and chalcophile elements are depleted in the BSE and BSM compared to lithophile elements with similar condensation temperatures, due to their incorporation into the metallic cores (Fig. 4). The abundances of siderophile elements in the BSE and BSM do not show a sub-parallel trend with that defined by lithophiles (Fig. 4). The degree of siderophile and chalcophile element depletion reflects a combination of planetary building block compositions and element fractionation processes during planetary accretion and differentiation (McDonough, 2014).

The BSE and BSM both have high concentrations and chondritic relative proportions of highly siderophile elements (HSE: Re, Os, Ir, Pt, Ru, Rh, Pd and Au; Fig. 4), which is at odds with any combination of high-pressure and temperature conditions for the partitioning of these elements into a core forming melt (Brandon et al., 2012; Walker et al., 2015; Day et al., 2016; Tait and Day, 2018). For example, core–mantle equilibration model in Martian interior (Righter et al., 2015) predicts sub-CI Re/Os and super-CI Ir/Os and Ir/Ru values in silicates, which are inconsistent with the chondritic HSE pattern in the BSM (Brandon et al., 2012; Tait and Day, 2018). In addition, Righter et al. (2015) assumes a high S concentration (>10 wt%) in the Martian core, which is much higher than a value predicted by the Martian volatility trend of lithophile elements (≤7 wt%; Yoshizaki and McDonough, 2020). These shared features of the HSE abundances in Earth and Mars are considered as evidence for late accretion of chondritic materials during the final stage (e.g., after ≥98% accretion) of planetary growth in the inner solar system (Kimura et al., 1974; Brandon et al., 2012; Day et al., 2016). Delivery of these HSE was also accompanied by an addition of volatile gases and fluids (H, C, N and O; Albarede, 2009; Alexander et al., 2012; Marty, 2012), although the late-accreted material to Mars might have been volatile-depleted (Wang and Becker, 2017; Righter et al., 2019).

On the other hand, the BSE is characterized superchondritic Ru/Ir and possibly Pd/Ir, which cannot be easily accommodated by the late addition of volatile-rich materials (Becker et al., 2006). Experimental studies showed that these high ratios in the BSE might reflect *P*, *T*, and composition-dependent changes in partitioning behaviors of Ru and Pd, and proposed no need for the late addition of these elements (Righter et al., 2008, 2018; Wheeler et al., 2011; Laurenz et al., 2016). Alternatively, these inconsistencies between the BSE and chondrites show an unrepresentative sampling of asteroidal materials in our meteorite collections (Walker et al., 2015).

The average, time-integrated, planet-scale redox condition (i.e., metal-silicate equilibrium) is recorded in the Mg# of its mantle, with the BSE and BSM having an Mg# of ~0.89 and 0.75–0.8, respectively, and its core mass fraction (i.e., Mars ~20% and Earth ~ 32%; Section 2.3). These attributes document Mars being more oxidized than Earth. In addition, Mars lacks depletion in redox-sensitive, nominally lithophile elements (i.e., V, Cr, and Mn), and its mantle has a lower Hf/W value (~3.5; Dauphas and Pourmand, 2011; Yoshizaki and McDonough, 2020), which contrast with those for Earth (Fig. 4). The more oxidized conditions for the Martian mantle are also indicated by mineralogy, trace element compositions and valence states of Fe and Eu in Martian

Table 1
Physical and chemical properties of Earth and Mars. Modeled values are in normal and reference values in italic fonts.

Observation	Unit	Crust	Mantle	Core	Bulk planet	Reference value
Earth						
Mass[a,b]	kg	3.12×10^{22}	4.00×10^{24}	1.94×10^{24}	5.972×10^{24}	*5.97218(60)* $\times$ *10^{24}*
Mean density[a,b,c]	kg/m^3	2800	4400	11870	5514	*5514(2)*
Moment of inertia[a]	–	1%	88%	11%	0.3308	*0.330690(9)*
Heat production (K, Th, U)[b,d,e,f]	TW	*7.3*	*12.6*	0	*19.9*	*46(3)*[g]
	pW/kg	232	3.1	0	3.3	–
Mars						
Mass[h]	kg	2.56×10^{22}	5.01×10^{23}	1.17×10^{23}	6.419×10^{23}	*6.417(3)* $\times$ *10^{23}*
Mean density[i]	kg/m^3	3010	3640	6910	3936	*3935(1)*
Moment of inertia[h]	–	7%	89%	4%	0.3638	*0.3639(1)*
Heat production (K, Th, U)[j,k,l]	TW	1.3	1.3	0	2.5	*2.7(2)*[g]
	pW/kg	49	2.5	0	3.9	–

Mantle + crust[d,k]			Core[d,k]			Bulk planet[d,k,m]		Chondrite[n]		
wt%	Earth	Mars	wt%	Earth	Mars	wt%	Earth	Mars	EH	L	CI
SiO_2	44.9	45.5	Fe	85.5	79.5	O	29.7	36.3	30.0	35.8	29.9
TiO_2	0.20	0.17	Ni	5.1	7.4	Fe	32.0	23.7	31.0	22.7	27.7
Al_2O_3	4.44	3.59	O	2	5.2	Mg	15.4	15.3	11.3	15.7	14.3
MnO	0.14	0.37	S	1.8	6.6	Si	16.1	17.4	17.8	19.5	16.0
FeO	8.06	14.7	H	0.06	0.9	Ni	1.82	1.4	1.87	1.27	1.58
MgO	37.8	31.0	Co	0.25	0.33	Ca	1.71	1.69	0.91	1.38	1.36
CaO	3.54	2.88	P	0.20	0.33	Al	1.59	1.56	0.86	1.29	1.26
Na_2O	0.36	0.59	Si	4	0	S	0.59	1.2	6.2	2.3	8.0
K_2O	0.034	0.043	Cr	0.75	0						
P_2O_5	0.021	0.17				Total	99.0	98.5	100	100	100
NiO	0.25	0.046	Total	99.7	100.2						
Cr_2O_3	0.15	0.88				Mg/Si	0.96	0.88	0.63	0.81	0.89
						Al/Si	0.10	0.09	0.05	0.07	0.08
K (ppm)	280	360				Fe/Si	2.0	1.4	1.7	1.2	1.7
Th (ppb)	76	68									
U (ppb)	20	18									
Total	100.2	99.9									

[a] Chambat et al. (2010).
[b] Wipperfurth et al. (2020).
[c] Dziewonski and Anderson (1981).
[d] McDonough (2014).
[e] Jaupart et al. (2015).
[f] Rudnick and Gao (2014).
[g] Global surface heat loss.
[h] Konopliv et al. (2016).
[i] Rivoldini et al. (2011).
[j] Taylor and McLennan (2009).
[k] Yoshizaki and McDonough (2020).
[l] Parro et al. (2017).
[m] This study.
[n] Alexander (2019a,b) (Volatile-free, normalized to total = 100 wt%).

meteorites. The Martian mantle, however, as recorded in Martian meteorites, shows a heterogeneous redox state (e.g., Herd et al., 2001, 2002; Wadhwa, 2001, 2008; Goodrich et al., 2003; McCanta et al., 2009; Shearer et al., 2011; Righter et al., 2016; Herd, 2019). Oxygen might be one of the light elements in the Earth's core (Ohtani and Ringwood, 1984), but its limited solubility in iron liquids at high P–T conditions (O'Neill et al., 1998) indicates small effects of the core formation in the BSE's Mg#, and supports the more reduced state of the BSE as compared to the BSM.

Earth and Mars have similar "upper mantle" mineralogies (Fig. 5). Both contain olivine, ortho- and clino-pyroxenes, and garnet, with the Earth's mantle being richer in olivine than the Martian mantle (~60% and ~45% in modal proportion, respectively). Differences in composition (Table 1) and interior thermal gradient (Breuer and Spohn, 2003; Katsura et al., 2010) of Earth and Mars results in different depths of the olivine-wadsleyite and wadsleyite-ringwoodite phase transitions. For Earth, these transitions are at 410 km and 520 km depth, respectively, and in Mars, they occur at 1000 km and 1300 km depth, respectively. These phase transitions are sharper in the Earth's mantle than the Martian mantle, because of the former's higher Mg#, greater garnet abundance, and hotter temperature (Frost, 2003; Filiberto and Dasgupta, 2011; Putirka, 2016). The Martian mantle might not have a layer of bridgmanite, which is a dominant phase in the Earth's lower mantle (Fig. 6).

2.2.2. *Heat producing elements (HPE)*

The rocky planets are powered by both primordial accretion energy (and lesser amounts from core formation) and radiogenic heat by radioactive decays of heat producing elements (HPE: K, Th, U). All three of the HPE are incompatible, lithophile elements that have been excluded from their cores and concentrated into planetary crusts (e.g., Corgne et al., 2007; Blanchard et al., 2017; Wipperfurth et al., 2018), which is beneficial for carrying out remote gamma-ray surveys of planetary surfaces (e.g., Peplowski et al., 2011; Surkov et al., 1987; Prettyman et al., 2015). The Martian crust is thicker (estimated to be 30–60 km thick with an average value of ~50 km; Zuber et al., 2000; McGovern et al., 2002; Wieczorek and Zuber, 2004; Humayun et al., 2013), less enriched in incompatible elements, and contains ~50% of the HPE budget of Mars, whereas Earth has a thinner, more chemically evolved crust, which contains only ~35% of the planet's HPE budget (Table 1 and Section A.2; Rudnick and Gao, 2014). Mars' internal heating Rayleigh number of $>10^5$ (Section A.3) is consistent with a

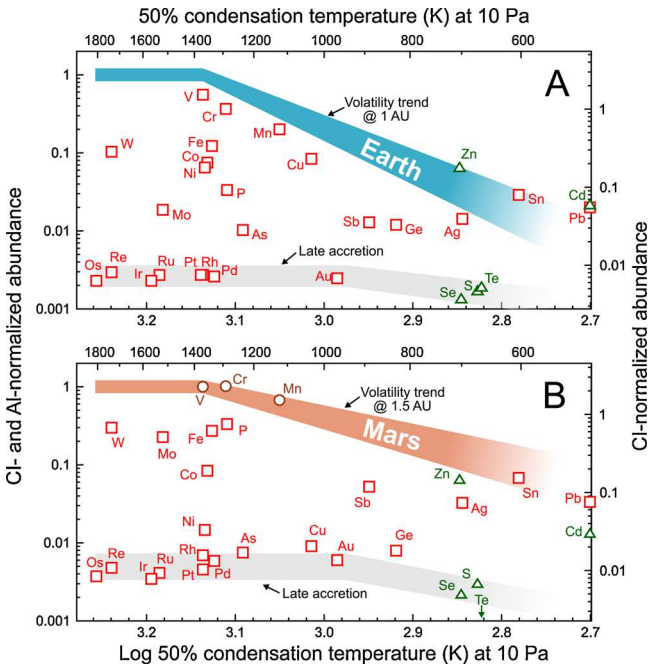

Fig. 4. Siderophile (red square) and chalcophile (green triangle) element abundances in the bulk silicate Earth and Mars plotted against 50% condensation temperature (K) of elements at 10 Pa (Wood et al., 2019). The values for *y* axes follow the same convention as Fig. 3. Also shown are time-integrated planetary volatility trends at 1 AU (Earth) and 1.5 AU (Mars) defined by lithophile elements (Fig. 3). Data sources are as in Fig. 1.

convecting Martian mantle and a dynamically stabilized Tharsis bulge (McKenzie et al., 2002; Kiefer, 2003).

With nearly a factor of 2 greater surface to volume ratio for Mars than Earth, the former cooled much faster (Filiberto and Dasgupta, 2011; Baratoux et al., 2011, 2013; Filiberto, 2017; Breuer and Moore, 2015; Putirka, 2016). Mars' surface heat flux is 19 ± 1 mW/m^2 (Parro et al., 2017) (cf., Earth's average is 90 mW/m^2; Jaupart et al., 2015), equivalent to a global heat flux of 2.75 ± 0.15 TW, of which 2.5 TW comes from radioactive decay (Table 1 and Section A.2). Mars' planetary Urey ratio (*Ur*: total radioactive heat production relative to total surface heat loss) is 0.92 ± 0.05, which is higher than that estimated for Earth (0.43) and its mantle Ur_{Mars} (planetary Ur_{Mars} minus the crustal fraction) is 0.8, more than double of that of the Earth's mantle (0.33). The high Ur_{Mars} demonstrates a minor contribution from secular cooling to the total Martian heat flux. Importantly, the modeled Martian surface heat flow varies between 14 and 25 mW/m^2 (Parro et al., 2017). A direct measurement the Martian surface heat flux by NASA's Interior Exploration using Seismic Investigations, Geodesy and Heat Transport (InSight) mission (Banerdt et al., 2020) will provide important constraints on its heat production and thermal history.

2.3. Core

The mantles of both Earth and Mars are depleted in siderophile and chalcophile elements due to core extraction (Fig. 4). Their core compositions are modeled using the following constraints: the planet's chondritic Fe/Ni value, temperature, mass, density, MOI, and for Earth, seismic profile (see McDonough, 2014; Yoshizaki and McDonough, 2020). Also, based on iron meteorite mineralogy (Scott and Krot, 2014) and cosmic abundance of elements (Lodders, 2020), planetary cores might contain sulfides, carbides and phosphides, and possibly other phases (e.g., silicides if formed under highly reduced conditions).

The Earth's core (32% by mass) has an outer liquid layer and a solid inner core (~5 wt%) (Fig. 6). Estimates of the size of the Martian core

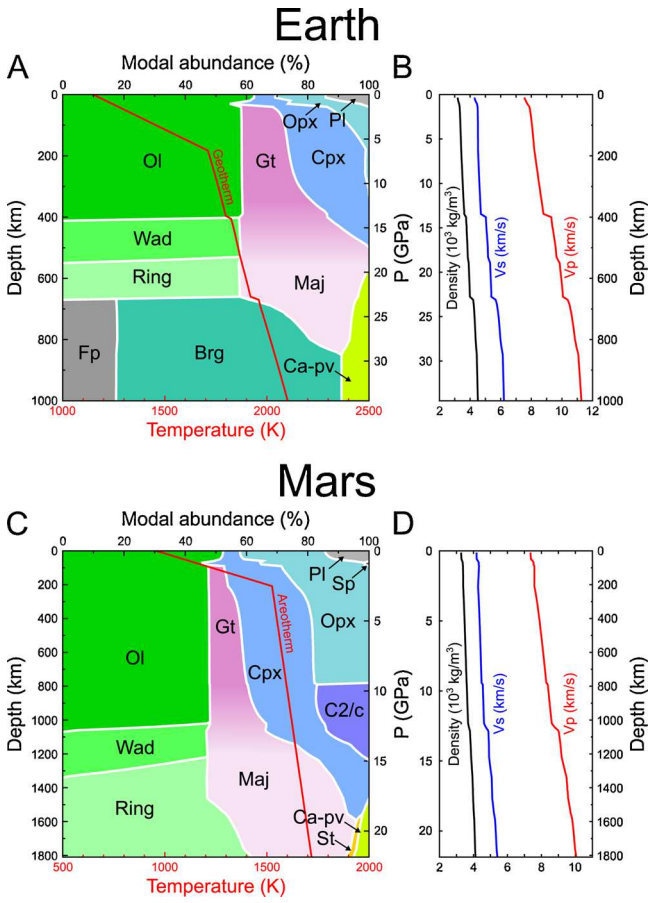

Fig. 5. Mineralogy and physical properties of planetary mantles. (A, C) Phase transitions and (B, D) P- and S-wave velocities and density from surface to the core-mantle boundary in the Earth's and Martian mantle. Red lines show temperature profile in the mantle. Figures for Earth are based on the mantle compositional model of McDonough (2014) and model geotherm from Katsura et al. (2010). Figures for Mars are reprinted from T. Yoshizaki and W.F. McDonough (2020) The composition of Mars, Geochimica et Cosmochimica Acta 273, 137–162, Copyright (2020), with permission from Elsevier. Abbreviations: Brg, bridgmanite; Ca-pv, Ca-perovskite; Cpx, clinopyroxene; C2/c, high-pressure clinopyroxene; Fp, ferropericlase; Gt, garnet; Ol, olivine; Opx, orthopyroxene; Pl, plagioclase; Ring, ringwoodite; Sp, spinel; St, stishovite; Wad, wadsleyite.

ranges from 18–25 wt% and 1500–1900 km, respectively (Section A.1.3). Data from multiply orbiting satellites provide a precise (±2%) measure of Mars' Love number solution (k_2) and document a possible existence of a partially molten core (Yoder et al., 2003; Genova et al., 2016; Konopliv et al., 2016). This observation indicates significant amounts of light elements in the core that lowers its solidus temperature.

Sulfur is a prime candidate for light elements in a planetary core. The volatile element depletion trends for both Earth and Mars (Fig. 4) constrain the core's S content of ~1.8% in Earth and ~7% in Mars (Yoshizaki and McDonough, 2020; see also Sections A.1.2 and A.1.3). Since the estimated S contents of the Earth's and Mars' core are not high enough to explain their respected core density deficits, additional light elements in these cores are needed (e.g., Si, O, H and C). The additional light elements are likely to be different in these cores because metal-silicate partitioning behavior of elements depends on conditions of core formation (e.g., timing, *P*, *T*, f_{O_2}) and compositions of coexisting silicate and metallic phases.

As described above, a planet's volatility trend sets expectations for the absolute amount of siderophile and chalcophile elements in the planet and defines the proportion of these elements that were partitioned into the core. The degree of depletion below the volatility trend

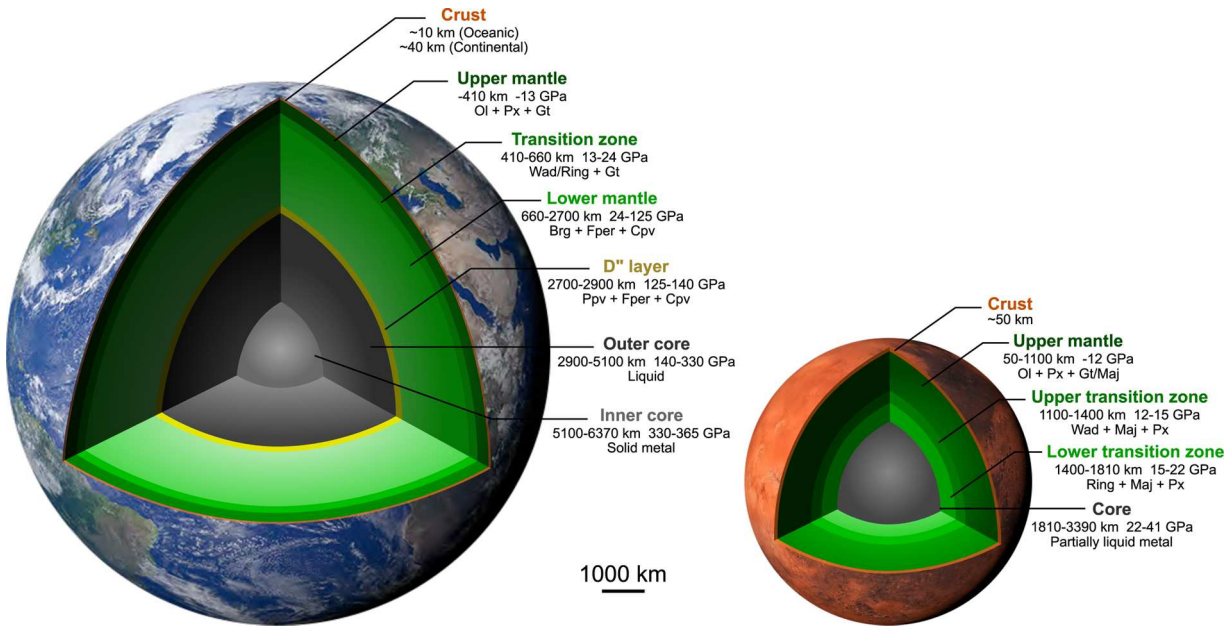

Fig. 6. Interior structure of Earth and Mars. Abbreviations: Ol, olivine; Px, pyroxene; Gt, garnet; Wad, wadsleyite; Ring, ringwoodite; Brg, bridgmanite; Cpv, Ca-perovskite; Ppv, post-perovskite; Fper, ferropericlase. The Mars figure is reprinted from T. Yoshizaki and W.F. McDonough (2020) The composition of Mars, Geochimica et Cosmochimica Acta 273, 137–162, Copyright (2020), with permission from Elsevier.

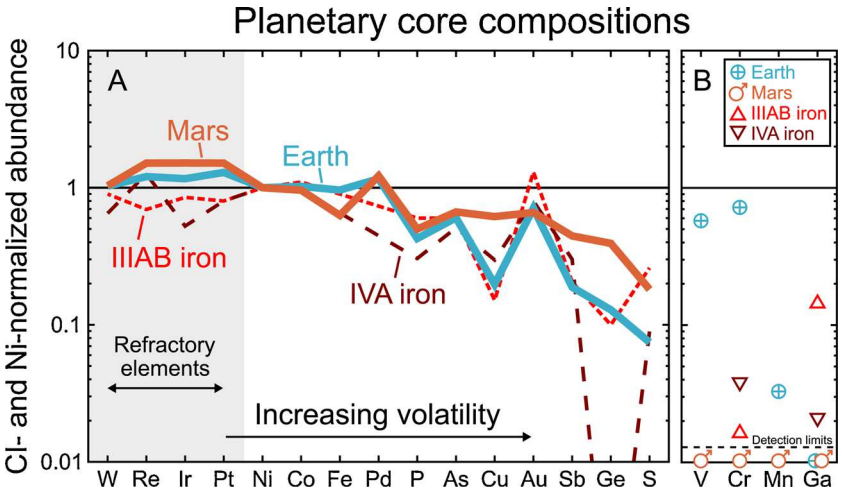

Fig. 7. Composition of metallic cores of Earth (McDonough, 2014), Mars (Yoshizaki and McDonough, 2020) and NC-group iron meteorite parent bodies (Wasson and Richardson, 2001; Chabot, 2018). (A) Siderophile and chalcophile element and (B) nominally lithophile element abundances. Elemental abundances are normalized to CI chondrite composition and Ni. Elements are arranged by their 50% nebular condensation temperatures (Wood et al., 2019), while W and Re are replaced to highlight chondritic highly siderophile element abundance in planetary cores. Type IIIAB and IVA iron meteorites have fractional crystallization (i.e., magmatic) origin and are isotopically classified as NC group meteorites (Burkhardt et al., 2011; Kruijer et al., 2017a; Poole et al., 2017).

defines an element's empirically established metal/silicate partition coefficient (McDonough, 2014; Yoshizaki and McDonough, 2020). The Martian core is enriched in siderophile and chalcophile MVE (e.g., P, Ge, S) as compared to the Earth's, and there appears to be little to no Ga in the cores of terrestrial planets, which contrasts with that seen in iron meteorite compositions (Figs. 7 and 8). Compared to the Earth's core, the Martian core is smaller, it might contain larger amounts of H and O, and it has a lower Fe/Ni value, with its mantle being enriched in Fe (Table 1). Overall, these factors contribute to Mars' lower uncompressed density as compared to the Earth's (3750 vs 4060 kg/m^3; Table 1). There is no unique model for core compositions of Earth and Mars that satisfies the geodetic and geochemical constraints (McDonough, 2014; Yoshizaki and McDonough, 2020), and further experimental and theoretical efforts are needed to constrain the light element budget in the planetary cores.

3. Discussion

3.1. Origin of volatile depletion in terrestrial planets

From Mercury to Mars and beyond to Vesta, the second biggest asteroid, their surface K/Th values are significantly lower relative to chondrites (Surkov et al., 1987; Taylor et al., 2006; Peplowski et al., 2011; Prettyman et al., 2015). The origins of this depletion and that of other MVE remain elusive, with possible explanations including post-nebular volatile loss due to internal or impact-induced heating (e.g., O'Neill and Palme, 2008; Norris and Wood, 2017) and incomplete condensation of nebular gas (e.g., Palme and O'Neill, 2014; Siebert et al., 2018). Since planetary K/Th ratios and relative amounts of more refractory olivine (Mg_2SiO_4) and less refractory pyroxene ($MgSiO_3$) do not correlate with their heliocentric distances in both the solar and extra-solar systems (e.g., Fig. 2A; van Boekel et al., 2004; Kessler-Silacci et al., 2006; Bouwman et al., 2008, 2010; Sargent et al., 2008), these volatile depletions do not solely reflect an outward temperature

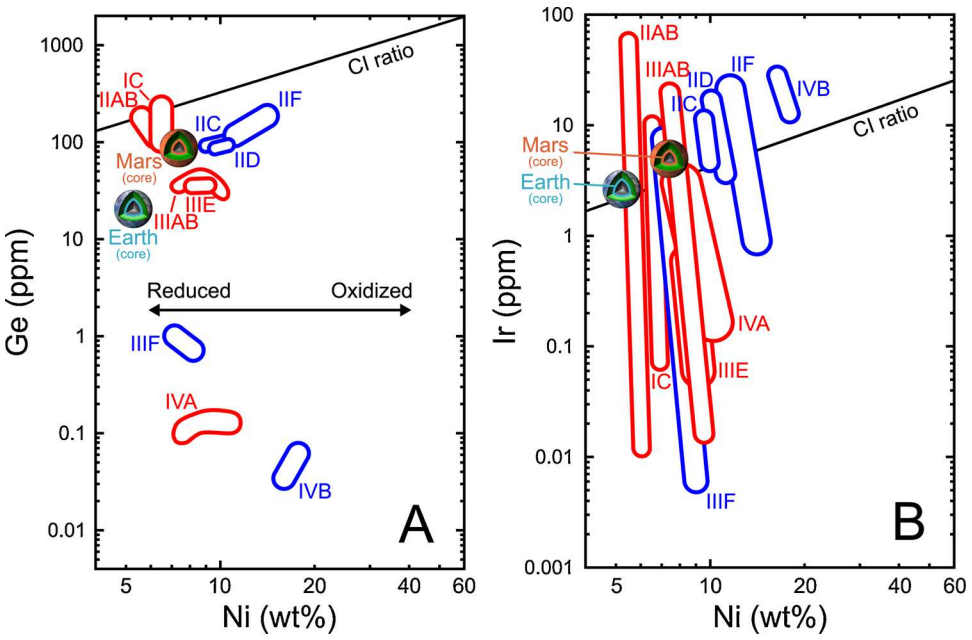

Fig. 8. Composition of metallic cores of Earth (McDonough, 2014), Mars (Yoshizaki and McDonough, 2020) and fractionally crystallized (i.e., magmatic) iron meteorites (Goldstein et al., 2009). (A) Ge versus Ni. (B) Ir versus Ni. Iron meteorites are classified into non-carbonaceous (NC: in red) and carbonaceous (CC: in blue) groups based on their Mo and W isotopic compositions (Burkhardt et al., 2011; Kruijer et al., 2017a; Poole et al., 2017). Silicate-bearing (non-magmatic) iron groups are not shown. The IIG iron meteorites are also excluded from the plot because isotopic data to classify them into NC or CC group are not available. CI chondritic ratios are from Lodders (2020).

decrease in the protoplanetary disk. The absence of heavy isotope enrichment in rocks from Earth and Mars for multiple isotope systems (e.g., K, Zn, Rb, Fe, Cd; Humayun and Clayton, 1995; Nebel et al., 2011; Paniello et al., 2012a; Sossi et al., 2016, 2018; Pringle and Moynier, 2017; Wombacher et al., 2008) indicates negligible post-accretionary evaporative loss of the MVE. In contrast, isotopically heavier siderophile or chalcophile compositions (e.g., Fe, Ga, Sn) of terrestrial and lunar mantles might reflect (1) core-mantle differentiation, (2) evaporation of the giant impactor's core and addition of the metal/sulfur-loving elements to the terrestrial mantle during the giant impact (see Section 3.3), or (3) planetary surface processes (e.g., Poitrasson et al., 2004; Kato and Moynier, 2017; Creech and Moynier, 2019). The ^{53}Mn-^{53}Cr and ^{87}Rb-^{87}Sr isotope systematics of meteorites and terrestrial samples are consistent with a volatility-dependent, gas--solid fractionation during first few Myr of the solar system (e.g., Shukolyukov and Lugmair, 2006; Trinquier et al., 2008; Hans et al., 2013; Moynier et al., 2012), which might be prior to the dissipation of the nebular gas (~t_0 + 5 Myr; Wang et al., 2017).

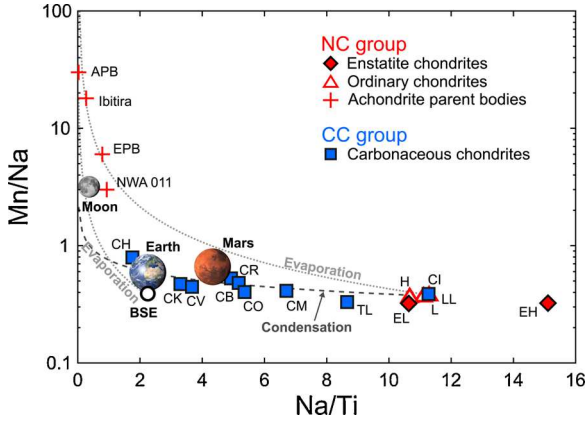

Fig. 9. Na/Ti vs Mn/Na in chondrites (Alexander, 2019a,b), differentiated asteroids (O'Neill and Palme, 2008), Moon (Dauphas et al., 2014), Earth (this study; McDonough, 2014; Siebert et al., 2018) and Mars (Yoshizaki and McDonough, 2020). Dark gray line shows incomplete condensation from a gas of CI composition. Light gray lines correspond to evaporative loss of Na and Mn from CI and the bulk silicate Earth (BSE) compositions, respectively. See Section A.1.1 for details of model calculations.

There is negligible evidence for post-accretionary MVE losses in the chemical compositions of these planets. The bulk Earth and Mars, together with chondrites, show negligible evidence of evaporative losses in ratios of Na, Mn and Ti (Fig. 9 and Section A.1.1; O'Neill and Palme, 2008; Siebert et al., 2018), which have distinct relative volatilities during condensation and evaporation. Values of Mn/Na and Na/Ti in the bulk Earth, Mars and chondrites are consistent with an incomplete nebular condensation, in which earlier condensates are removed from a nebular gas before a completion of more volatile species (e.g., Larimer, 1967; Larimer and Anders, 1967) (cf. O'Neill and Palme, 2008). The plot of Mn/Na versus Na/Ti indicates that a formation of precursors of Earth and Mars at higher temperatures than their isotopically linked counterparts (enstatite and ordinary chondrites, respectively), which is also suggested by the former's higher Mg/Si (i.e., olivine/pyroxene), Al/Si, and Al/Mg ratios (Kerridge, 1979; Larimer, 1979; Dauphas et al., 2015; Morbidelli et al., 2020).

Collectively, the compositions of rocky planets, as compared to their chondritic relatives, likely reflects volatility-dependent chemical fractionation in the protoplanetary disk, rather than the post-accretionary losses of MVE. In contrast, small differentiated asteroids (e.g., parent bodies of Eucrite and Angrite) show clear evidence for preferential loss of MVE (Fig. 9; O'Neill and Palme, 2008) and heavy isotope enrichment (e.g., Paniello et al., 2012b; Pringle et al., 2017; Tian et al., 2019), which are the hallmarks of evaporative losses during or after accretion. Volatile elements might have escaped from these small bodies during and/or after their accretion, due to their weak gravity field.

3.2. The building blocks of the terrestrial planets

The planetary building blocks appeared to be made up of high-temperature materials, dominantly chondrules, which are silicate droplets formed by transient heating events within first few Myr of the solar system evolution (Connelly et al., 2012; Bollard et al., 2017), and are an essential component of chondrites (e.g., Scott and Krot, 2014; Russell et al., 2018). MVE composition of chondrules provides a record of incomplete nebular condensation rather than evaporation processes (Humayun and Clayton, 1995; Alexander et al., 2000, 2008; Galy et al., 2000; Pringle et al., 2017). The refractory element enrichment and MVE depletion in the BSE and BSM are comparable to those observed for chondrules from carbonaceous chondrites (Fig. 10; Hewins and

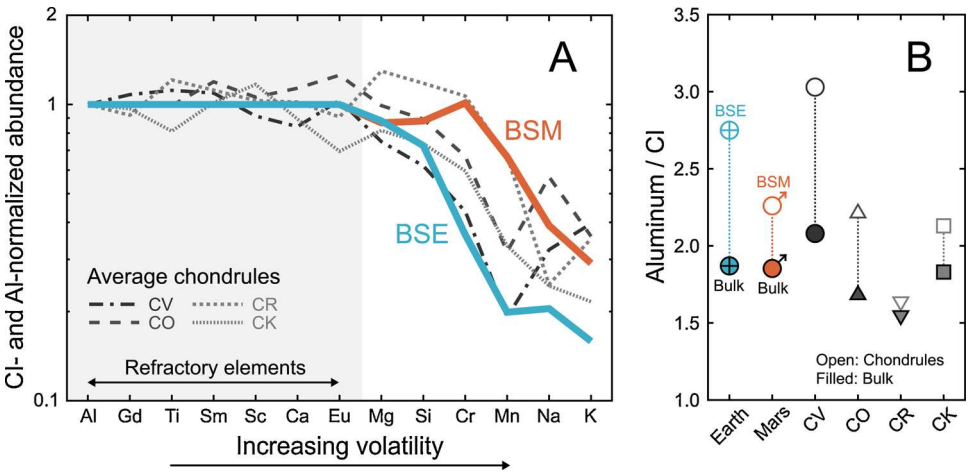

Fig. 10. Lithophile element composition of Earth, Mars, and carbonaceous chondrites and their components. (A) Lithophile element abundance in the bulk silicate Mars (BSM), bulk silicate Earth (BSE) and bulk chondrules from carbonaceous chondrites. Elemental abundances are normalized to CI chondrite composition and Al. Elements are arranged by their 50% nebular condensation temperatures. (B) CI-normalized Al abundances in the BSE, BSM, bulk planets, bulk chondrules and bulk chondrites. Chemical composition of chondrules is from Hezel et al. (2018b) and MetBase (2019). Other data sources are as in Fig. 1.

Herzberg, 1996; Mahan et al., 2018). Significantly, mass-dependent Ca (Huang et al., 2010; Magna et al., 2015; Amsellem et al., 2017; Simon et al., 2017; Bermingham et al., 2018) and Mg (Bizzarro et al., 2004; Young and Galy, 2004; Wiechert and Halliday, 2007; Bouvier et al., 2013; Olsen et al., 2016; Hin et al., 2017) isotopic compositions of chondrules, BSE and BSM also suggest that they inherited fractionated isotopic signatures from similar precursor materials, which have experienced high-temperature gas–solid fractionation processes.

Recent theoretical models of planetary growth favor formation of terrestrial planets via accretion of chondrule-sized pebbles (e.g., Johansen et al., 2015a,b; Levison et al., 2015). These models predict a rapid accretion of Mars-sized bodies under the presence of a nebular disk. Thus, Mars, with a $\tau_{\text{Mars}}^{\text{accretion}}$ of ~2 Myr (Dauphas and Pourmand, 2011; Kruijer et al., 2017b; Bouvier et al., 2018) (cf. Marchi et al., 2020), formed within the nebular disk lifetime (~5 Myr; Wang et al., 2017), whereas Earth is suggested to have $\tau_{\text{Earth}}^{\text{accretion}}$ ≥30 Myr (e.g., Kleine et al., 2009), which documents its accretion stretched beyond the lifetime of the nebular disk.

Differences in planetary MVE abundances (Fig. A.3) likely reflect aspects of their accretion histories and sizes. Chondrites, the least MVE-depleted bodies' materials, contain fine-grained, volatile-rich matrix that accounts for the largest fraction of the inventory of volatiles (e.g., Alexander, 2005, 2019a,b; Bland et al., 2005; Zanda et al., 2018). Although a relationship between chondrules and matrix remains poorly understood, their coexistence in the protoplanetary disk before planetesimal accretion is accepted (e.g., Hezel et al., 2018a; Zanda et al., 2018). Some carbonaceous chondritic asteroids accreted more chondrules and less matrix, resulting in more MVE-depleted compositions (Figs. 11B and A.4). According to the pebble accretion model (Johansen et al., 2015a,b; Levison et al., 2015), planetesimal growth starts off by preferentially accreting the smallest particles, and as the body grows, it prefers to accrete larger and larger size particles. This mechanism would lead to a growing planetesimal having a larger chondrule/matrix ratio, and becoming more MVE-depleted as its mass increases. Thus, small chondritic asteroids likely co-accreted chondrules and matrix, whereas Mars, with its intermediate volatile depletion, size and accretion timescale, likely accreted a greater fraction of chondrules to matrix (Fig. 11). Finally, the Earth's prolonged accretion history was dominated by chondrule accretion, resulting in its significant MVE-depleted composition. The MVE depletion scales with size of the chondritic parent body and planet (Fig. 11), implying an accretion driven process from an undepleted nebula (i.e., CI (solar) composition). Exceptions are small differentiated bodies (e.g., the Moon and Vesta) that experienced post-nebular volatile loss due to internal or impact-induced heating (Section 3.1). Thus, the chondrule-driven planetary growth plays a critical role in establishing the planetary MVE-depleted characteristics.

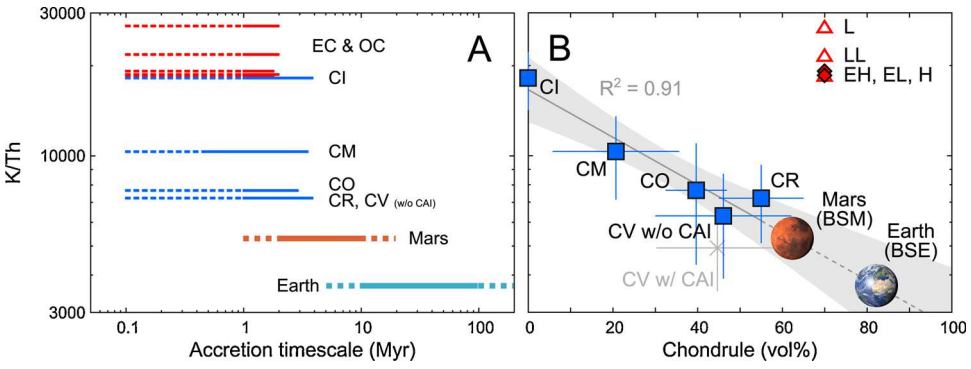

Fig. 11. (A) Accretion timescale (Myr) vs K/Th ratio of chondrites and terrestrial planets. Duration of accretion of chondritic asteroids is based on the Pb–Pb, Hf–W and Al–Mg ages of chondrules (Amelin et al., 2002; Amelin and Krot, 2007; Connelly et al., 2008, 2012; Connelly and Bizzarro, 2009; Bollard et al., 2017, 2019; Villeneuve et al., 2009; Nagashima et al., 2017; Schrader et al., 2017; Kita et al., 2013; Pape et al., 2019; Budde et al., 2016, 2018), Mn–Cr ages of asteroidal secondary alteration products (Fujiya et al., 2012; Doyle et al., 2015), and thermal modeling of asteroids (Sugiura and Fujiya, 2014). Accretion timescales of Earth and Mars are defined based on Kruijer et al. (2017b, 2020), Kleine et al. (2009), Dauphas and Pourmand (2011), Kruijer et al. (2017b), and Connelly et al. (2019). (B) Abundance of chondrules (vol%) vs K/Th value of chondrites. Error bars (shown only for carbonaceous chondrites) represent 2 standard deviations, and gray area corresponds to the 95% confidence interval of the linear regression. The abundances of chondrules in chondrites are based on McSween (1977a), McSween (1977b), McSween (1979) and Scott and Krot (2014). The amounts of chondrules in Earth and Mars are estimated based on their K/Th values and extrapolation of the carbonaceous chondritic trend. Section A.4 for a method to calculate the CAI-free bulk CV composition.

In contrast, enstatite and ordinary chondrites, whose isotopic composition and redox state are most related to Earth and Mars, respectively (e.g., Fig. 2B Trinquier et al., 2007, 2009; Warren, 2011; Dauphas, 2017), do not show a clear refractory enrichment nor MVE depletion (Figs. 2A, 11 and A.4). In addition, chondrules from these NC chondrites are less depleted in MVE than the BSE and BSM (Fig. A.5). Thus, the chondrule-driven MVE-depletion scenario discussed above cannot be applied to the NC chondrites we have in our collections. These observations indicate that the NC chondrites represent refractory-poor, volatile-rich counterparts of the inner rocky planets. Morbidelli et al. (2020) showed that the low Mg/Si and Al/Si solids, which are comparable to those of NC chondrites (Fig. 2A), condense after removal of early-formed, high-temperature condensates from the system.

Differences in the timing of planetary accretion might also be important in establishing their relative abundances of MVE. Chronology of meteorites combined with thermal modeling of asteroids (Sugiura and Fujiya, 2014; Kruijer et al., 2017a; Zhu et al., 2020) indicates that the undifferentiated NC planetesimals accreted 1–2 Myr after formation of differentiated NC bodies (i.e., iron meteorite parent bodies and terrestrial planets). The variation in the absolute ages of chondrules (Connelly et al., 2012; Bollard et al., 2017), occurrence of relict grains (Jones, 1994; Weisberg et al., 2011; Tenner et al., 2018) and igneous rims (Krot and Wasson, 1995) in chondrules, and the presence of compound chondrules (Wasson et al., 1995) indicate that chondrule formation was a repeated event. Thus, the longer chondrules remained in the accretionary disk, the more opportunities it has being recycled by later events. Ordinary chondrite chondrules records an admixing of MVE-rich CC-like materials to MVE-poor chondrule precursors into the NC reservoir (Mahan et al., 2018; Schiller et al., 2018; Bollard et al., 2019). Additions of MVE-rich materials and repeated chondrule recycling produce younger chondrules with higher MVE abundance (Mahan et al., 2018). Thus, terrestrial planets, which are dominated by earlier materials that experienced fewer recycle events and MVE addition, are more depleted in MVE as compared to the NC chondrites, which accreted the younger MVE-enriched chondrules.

In contrast, chondrule formation scenarios predict less frequent chondrule formation/recycle events in the outer solar system (e.g., Morris et al., 2012; Johnson et al., 2015; Sanders and Scott, 2018; Pilipp et al., 1998). This prediction is consistent with chemical and isotopic signatures of CC chondrules (e.g., Hewins and Zanda, 2012; Tenner et al., 2018; Mahan et al., 2018). Consequently, the CC chondrules could have preserved their MVE depletion until the accretion of CC chondritic asteroids, and thus are chemically comparable to the early NC materials which formed the inner rocky planets.

This chondrule-rich accretion model for the terrestrial planets reveals the limited ability to reach greater levels of enrichment in refractory elements (Figs. 2A and 10 B), which is a concern for planetary compositional models promoting high refractory element abundance (Section 2.1). To reach higher levels of refractory element enrichment beyond that seen in CV chondrites and their chondrules, larger amounts of refractory inclusions are needed, which is inconsistent with chondritic REE ratios of the BSE (Stracke et al., 2012; Dauphas and Pourmand, 2015).

3.3. Formation models of the terrestrial planets

3.3.1. Previous models of the Earth's accretion and Moon formation

Depletion of moderately to highly siderophile and chalcophile elements in the BSE is consistent with Earth's initial accretion from highly reduced, volatile-depleted materials, that was later oxidized by volatile-rich additions (e.g., Wänke, 1981; Wänke et al., 1984; Wänke and Dreibus, 1988; O'Neill, 1991; Rubie et al., 2011, 2015). Support for this temporal evolution in volatile accretion is found in multiple radiogenic isotope systems (e.g., Rb-Sr, U-Pb, Ag-Pd, I-Pu-Xe; Halliday and Porcelli, 2001; Albarede, 2009; Schönbächler et al., 2010; Mukhopadhyay, 2012; Ballhaus et al., 2013; Maltese and Mezger, 2020), metal-silicate partitioning behaviors of elements such as W, Mo, S and C (e.g., Wade et al., 2012; Li et al., 2016; Suer et al., 2017; Tsuno et al., 2018; Ballhaus et al., 2017), and *N*-body simulations of planetary formation (e.g., Raymond et al., 2006; Morbidelli et al., 2012). However, the degree of volatile element depletion in the pre-impact proto-Earth remains unconstrained.

The two-component accretion models for the growth of Earth envisage mixing of highly reduced, volatile-depleted materials with oxidized, volatile-rich, "CI-chondritic" materials in some proportion, not well defined, but generally conceived their mass ratios to be in the range of 60:40 to 90:10 (Wänke et al., 1984; Wänke and Dreibus, 1988; O'Neill, 1991). Some mass estimates of the late oxidized addition are comparable to a Mars-sized, Moon-forming impactor (e.g., Canup and Asphaug, 2001; Canup, 2004, 2008). The impactor's composition has often been assumed to be CI-chondritic (e.g., O'Neill, 1991, 1991; Maltese and Mezger, 2020).

However, the CI-chondritic impactor model has been multiply challenged. The common MVE depletion in rocky differentiated bodies in the solar system (e.g., sub-solar K/Th ratios; Section 3.1) might indicate a similar MVE depletion in the Mars-sized impactor. In addition, the CI-like impactor model requires a significant volatile depletion in the proto-Earth, perhaps at levels seen in angrites and calcium-aluminum-rich inclusions (CAIs), which show heavy Mg- and Si-isotope enrichment and significant depletion of moderately volatile elements (e.g., Grossman et al., 2000, 2008; Pringle et al., 2014) due to significant evaporative losses of the major and more volatile elements by impact-induced or transient nebular heating events (e.g., Stolper and Paque, 1986; Richter et al., 2002; Pringle et al., 2014; Yoshizaki et al., 2019; Young et al., 2019). However, such isotopic signatures are not recognized for Earth (Section 3.1). Furthermore, models predicting compositional zoning in the protoplanetary disk have a region of CI-like material accreting at $\geq$15 AU (Desch et al., 2018), where it is predicted that the disk mass is too low to form a Mars-sized body.

Compositional similarities of Earth and Moon in multiple isotope systems set strict constraints on the nature of both the impactor and proto-Earth, that is, they are derived from a similar NC isotopic reservoir that appears to be restricted to inner solar system sources (e.g., Wiechert et al., 2001; Trinquier et al., 2009; Warren, 2011; Zhang et al., 2012; Greenwood et al., 2018; Dauphas, 2017; Kruijer et al., 2017a). This observation is consistent with dynamical simulations which predict low probabilities of a Moon-forming impactor originating from >10 AU (e.g., Jackson et al., 2018). Thus, these constraints exclude the isotopically distinct CI chondrite as an impactor candidate. In contrast, recent Mo and O isotopic data from a broad range of NC and CC materials challenge this exclusion and find support for a CC-like impactor and/or vigorous mixing of proto-Earth and impactor, requesting further constraints to reveal the origin of the Earth-Moon system (Young et al., 2016; Budde et al., 2019; Cano et al., 2020). Furthermore, the recently-proposed synestia model (Lock et al., 2018) has the Moon forming in a vapor cloud surrounding Earth. This vapor cloud was produced by a large impact, resulting in a well-mixed, chemically equilibrated proto-earth and the vapor cloud.

3.3.2. Mars-like Moon-forming giant impactor model

Here we propose a model for the origin of the Moon. Our model is a modification of the original Wänke et al. (1984)'s model and later modified by O'Neill (1991, 1991). In our version of this model, we envision the Earth's formational history in 4 steps and use a differentiated Mars-like composition (Yoshizaki and McDonough, 2020), instead of CI composition, for the giant impactor. Figs. 12 and 13 show the details of our model: Fig. 12 specifically highlights the differences between our model and those previously presented. Our model starts with

1 the accretion of the proto-Earth (reduced and volatile-depleted) accompanied by continuous core-mantle differentiation (~90% of Earth's mass),

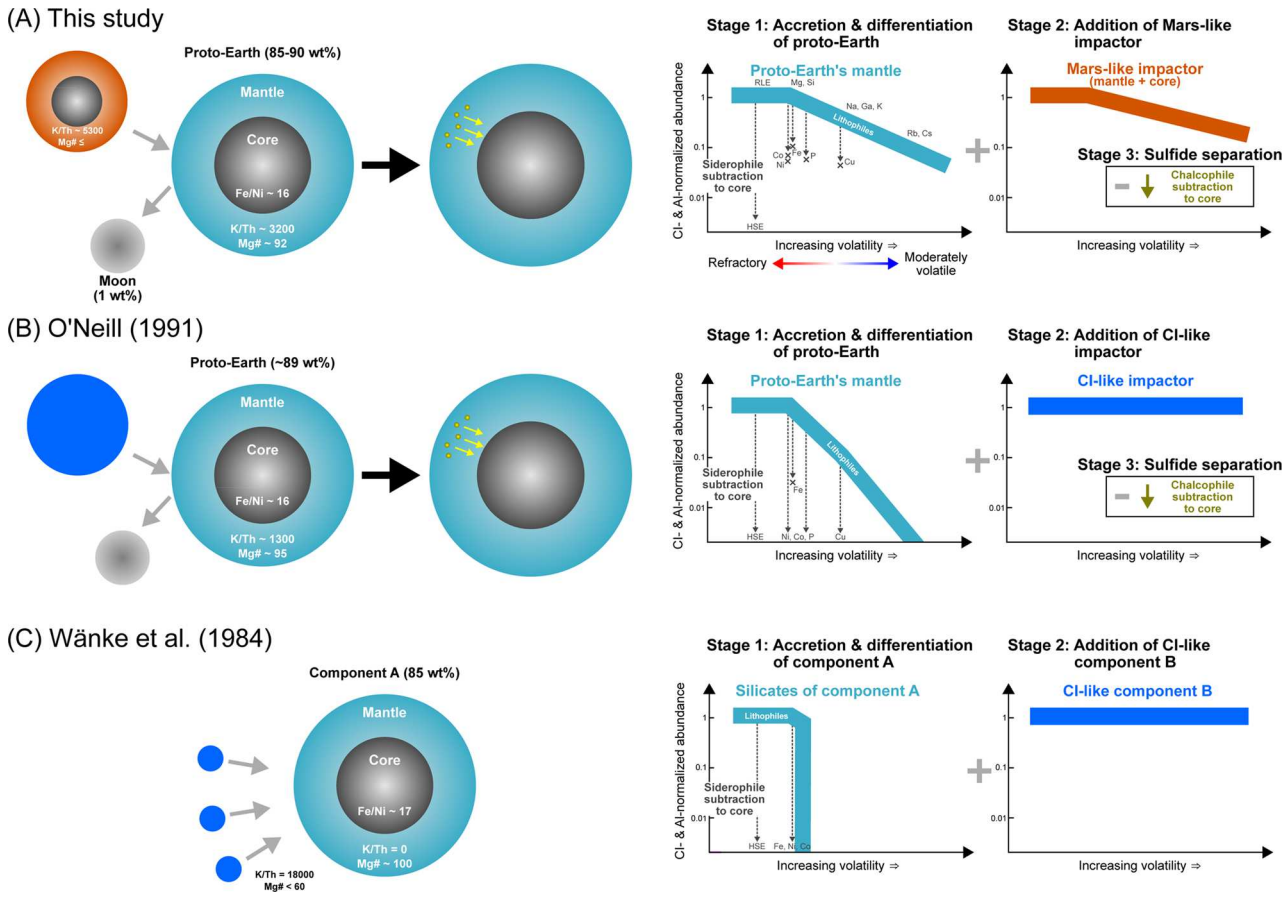

Fig. 12. A cartoon summarizing three models of the Earth's accretion: (A) this study; (B) O'Neill (1991); and (C) Wänke et al. (1984). The later models envisage Earth's formation as composed of four stages: (1) accretion and differentiation of a proto-Earth, (2) addition of a giant impactor to the proto-Earth's mantle, (3) loss of a sulfide matte from this mantle, and (4) late accretion of volatile-rich chondritic materials (not shown).

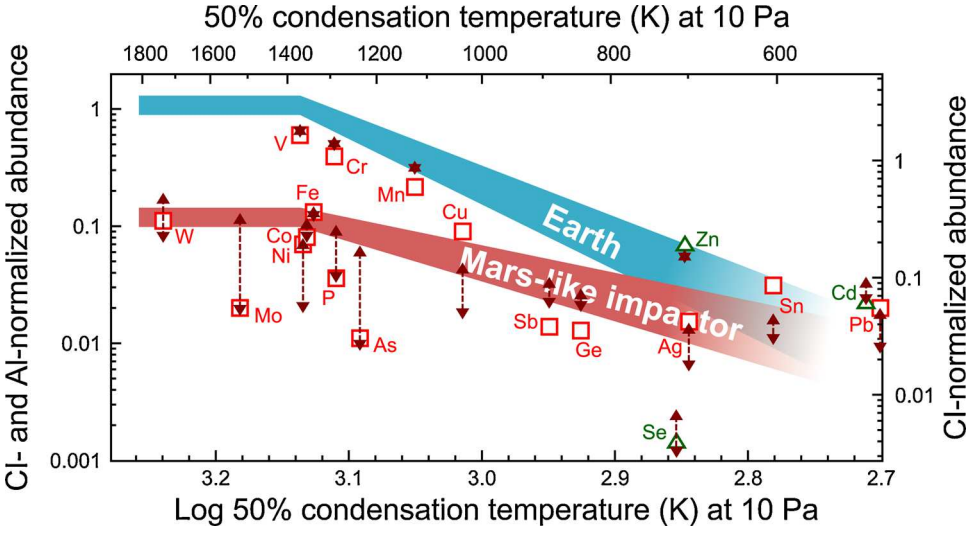

Fig. 13. Siderophile (red square) and chalcophile (green triangle) element abundances in the BSE, and a model BSE composition after the sulfide matte subtraction (dark red arrow) predicted by a Mars-like (i.e., size and composition) Moon-forming impactor scenario. The dark red arrows represent the model compositional range based on sulfide-silicate partition coefficients of elements (Table A.1). Highly siderophile and chalcophile elements are not shown, as their abundances in the present-day BSE can be explained by the late addition of volatile-rich materials (Step 4). Also shown are the Mars-like impactor's contribution (red band) in the present-day Earth composition (blue band). The values for x and y axes follow the same conventions as Fig. 4.

2 followed by a late-stage Moon-forming giant impact event (30–100 Myr after t_0; Kleine et al., 2009) that adds the final ~10% mass (oxidized and volatile-enriched) to Earth and forms a protolunar accretion disk,

3 subsequently, the mantle loses a Fe–Ni (±O) sulfide liquid (sulfide matte; O'Neill, 1991) to the core (~0.5% BSE mass),

4 and finally, the BSE receives the addition of (~0.5% of the BSE mass) a late accretion component that brings the highly siderophile and chalcophile elements in chondritic proportions and highly volatile gases and fluids (see Section A.5 for details of the modeling).

The addition of MVE by the impactor leads to sulfur saturation in the

magma ocean, generating an Fe–Ni (± O) sulfide liquid (post-impact sulfide matte; O'Neill, 1991; Rubie et al., 2016). The sulfide matte precipitates through a crystallizing mantle into the core due to its high immiscibility, low wetting angle, and high density (Gaetani and Grove, 1999; Rose and Brenan, 2001). Assuming that the sulfide matte, with a present-day mantle sulfide-like composition (Lorand and Conquéré, 1983), extracted all S from the post-impact Earth's mantle; its mass is estimated to be ~0.5 wt% of the present-day Earth's silicate mantle (Section A.5).

The siderophile and chalcophile element abundances of the BSE are reproduced when 10–15% of a planetary mass is added by the impactor and most of the impactor's core equilibrates with the proto-Earth's mantle (Fig. 13 and Section A.5). In this scenario, the bulk proto-Earth contains ≥80% of the present-day Earth's budget of most of the MVE (e.g., K/Th ~ 3200; Rb/Sr ~ 0.026; Table A.2), with the Mars-like impactor contributing a limited amount of MVE (Fig. 13). We envision the proto-Earth as having a MVE abundance comparable to that of chondrules (Figs. 10 and 11 B). Thus, the proto-Earth's composition is consistent with the chondrule-rich accretion scenario (Section 3.2) and requires no need for a post-accretionary loss of MVE from the proto-Earth before the Moon-forming event (Section 3.1).

The mass fraction of the impactor contributing to the lunar composition provides a critical constraint on the lunar formation models. The lunar mantle is depleted in nominally lithophile V, Cr and Mn (Dreibus and Wänke, 1979). Such lunar mantle depletion can be achieved by high-*T* or S-rich conditions during lunar core formation, but these conditions seem unlikely (Steenstra et al., 2016). If a Mars-sized impactor with no V, Cr or Mn-depletion in its mantle contributed >70% of Moon, as predicted by the canonical giant impact models (Canup and Asphaug, 2001; Canup, 2004, 2008), ≥40% of evaporative losses of Mn and Cr are needed to produce their depletion in the lunar mantle (Fig. 14). Such significant evaporation of these elements is inconsistent with their least volatile nature among MVE (Gellissen et al., 2019; Sossi et al., 2019). Thus, the proto-Earth's V, Cr and Mn-depleted mantle should be a primary source of the Moon-forming materials, as supported by their isotopic similarities (e.g., Wiechert et al., 2001; Warren, 2011; Zhang et al., 2012; Greenwood et al., 2018). A recent geochemical model of Earth's Moon formation and differentiation prefers a present-day BSE-like MVE composition for the bulk proto-Moon (i.e., lunar source materials before gas-melt fractionation; Righter, 2019), which is consistent with the proto-Earth's MVE abundance and its large contribution to the lunar source materials (Fig. 14 and Table A.2). The proto-Earth origin of the Moon is also consistent with recent particle hydrodynamic collision simulations (Hosono et al., 2019) which showed that a terrestrial magma ocean might be a source of lunar building blocks.

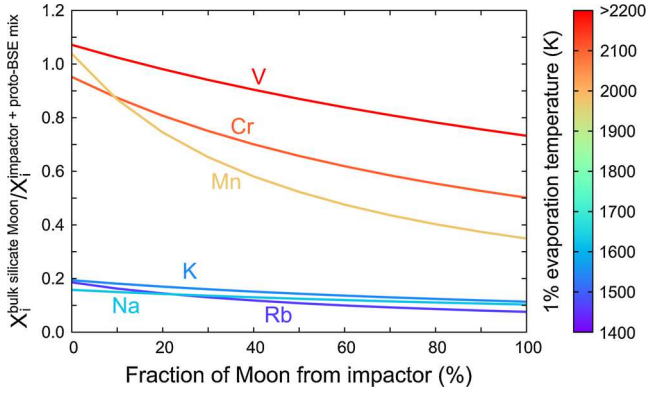

Fig. 14. Abundances of moderately volatile elements (X_i) in bulk silicate Moon and mixture of the Mars-like Moon-forming impactor's mantle and proto-BSE, plotted against mass fraction of the impactor in Moon. $X^{\text{bulk silicate Moon}_i}$ are based on Warren (2005), McDonough et al. (1992), and O'Neill (1991). Colors of curves correspond 1% evaporation temperatures of elements from a silicate melt at $logf_{O_2} = -10$ at 1 bar (Sossi et al., 2019).

3.3.3. *Mars' accretion and core formation*

Our compositional estimate of Mars requires a much simpler formation history as compared to Earth's multi-stage formation scenario. The lack of depletion in nominally lithophile elements in the BSM (V, Cr, and Mn; Fig. 4) is consistent with its accretion under uniformly oxidized and low-*T* conditions (e.g., Wood et al., 2009). Mars might have experienced a large impact(s) that produced its hemispheric crustal dichotomy and possibly Martian moons (e.g., Marinova et al., 2008; Canup and Salmon, 2018), but estimates of a putative small impactor (~0.1% of the Mars' mass; Canup and Salmon, 2018) would result in negligible changes in its bulk composition. The 0.5–1% mass addition of chondritic late accretion material provides highly siderophile and chalcophile elements to the Martian mantle (Tait and Day, 2018; Yoshizaki and McDonough, 2020).

Righter and Chabot (2011) and Yang et al. (2015) estimated Martian core formation happening at 14 ± 3 GPa and 2100 ± 200 K based on its previous compositional models. Following the approaches of Righter and Chabot (2011) and Yang et al. (2015), the Martian siderophile element distribution of Yoshizaki and McDonough (2020) can be modeled by single stage *P–T* and redox conditions (Fig. A.8), whereas there is no unique solution for Martian core formation (Fig. A.9).

The simple formation history of Mars, combined with its rapid and early accretion (Dauphas and Pourmand, 2011; Kruijer et al., 2017b; Bouvier et al., 2018; Marchi et al., 2020), is consistent with its status as a planetary embryo. Given compositional and redox state gradients in the protoplanetary disk, Mars might record the chemical characteristics of nebular materials in the Mars' orbit in the first few years of the solar system, whereas Earth might have incorporated oxidized materials from greater heliocentric distance in its later accretion stage (Section 3.3.2; Rubie et al., 2015). The Mars' status as a planetary embryo suggest that a Mars-sized body commonly has a Mars-like composition, supporting the Mars-like Moon-forming impactor scenario (Section 3.3.2).

3.4. *Conditions for a habitable planet formation*

The early $\tau_{\text{Mars}}^{\text{accretion}}$ age implies that Mars underwent global-scale silicate melting and rapid core formation due to heating from short-lived ^{26}Al and ^{60}Fe (Fig. A.12; Dauphas and Pourmand, 2011; McDonough et al., 2020). The peak radiogenic heating occurs at about 1 to 5 Myr after t_0, well within the time scale for Mars accretion. With $\tau_{\text{Mars}}^{\text{accretion}} = 2$ Myr, the radiogenic energy supplied by ^{26}Al is comparable to Mars' gravitational binding energy (~7×10^{29} J and ~10^{30} J, respectively). During the first 10 Myr, radiogenic heating (^{26}Al, ^{60}Fe and ^{40}K, in order of significance) is comparable to the planet's primordial energy and is a major control on its thermal evolution.

Mars has the attributes needed for a rocky planet to be biologically available in its early history (e.g., Ehlmann et al., 2016), and it has a higher bulk heat production than Earth's (3.9 vs 3.3 pW/kg; Table 1). Nonetheless, it has rapidly lost much of its primordial energy (i.e., accretion and core differentiation) due to its larger surface to volume ratio (a factor of 2) and smaller core size (i.e., reduced bottom heating), and it is in waning stages of limited fuel resources (Parro et al., 2017; Yoshizaki and McDonough, 2020). Basal heating of the Martian mantle by its core enhances its thermal evolution, while the transfer of hydrogen from the adjacent ringwoodite to the core (Shibazaki et al., 2009; Yoshizaki and McDonough, 2020) reduces the lifetime of the dynamo (O'Rourke and Shim, 2019). Collectively, these processes likely contributed to dynamo termination at ~4 Ga and loss of the protective magnetosphere (Acuña et al., 1999; Arkani-Hamed, 2004; Lillis et al., 2008). This magnetosphere shields the planet from atmospheric losses, enhances its surface UV radiation, and leads to dramatic climate changes (Ehlmann et al., 2016).

Volatile elements may play a critical role in establishing the amount of light elements in and solidus of the core. The amount of water and other volatile species in the planet's interior and surface may potentially create the appropriate conditions for the initiation of plate tectonics (e.g., Albarede, 2009; Ehlmann et al., 2016). Likewise, the heat-producing elements and a reduced core solidus keep the metallic core convecting and lead to the creation of a magnetic field, which shields a planet's surface from cosmic rays. Together, heat-producing and volatile elements regulate a planet's cooling history, drive crustal differentiation, and make it habitable (Ehlmann et al., 2016). The simple formation history of Mars (Section 3.3.3; Rubie et al., 2015) emphasizes the uniqueness of Earth, the sole habitable planet in our solar system. In turn, the Earth–Mars comparison indicates that high-temperature nebular chemical processes and timescales of planetary accretion are essential in making habitable planets.

Depletion in volatile elements appears to be a common feature of the terrestrial planets (Fig. 3; Surkov et al., 1987; Peplowski et al., 2011), and may likely be so for rocky exoplanets (Harrison et al., 2018, 2021). The relationship between the planetary volatile depletion, size, accretion timescale and abundance of chondrules (Fig. 11) predict accretion timescales of Venus and Mercury of 30–100 Myr and 2–10 Myr, respectively, based on their Earth- and Mars-like K/Th ratios, respectively (Surkov et al., 1987; Peplowski et al., 2011). The predicted ages of Mercury and Venus provide a foundation for future investigation of their thermal history and habitability.

Venus and Earth are quite similar in their physical and chemical properties (size, bulk K/Th ratio, Mg# in basalt and possibly MOI; e.g., Surkov et al., 1987; Dumoulin et al., 2017), but their present-day surface conditions are distinct. Venus does not show a clear evidence for a giant impact, and its size and K/Th ratio (~3000; Surkov et al., 1987) are comparable to those of the proto-Earth (K/Th ~ 3200; Table A.2). Therefore, the present-day Venus might be comparable to the pre-impact proto-Earth. Further observational, cosmochemical and theoretical investigations of Venus may provide useful insights into the pre- and post-formational history of Earth, the only habitable planet in the today's solar system.

4. Conclusions

The refractory element enhancement and volatile depletion of Earth and Mars were established by a nebular chemical fractionation. Post-accretionary losses of moderately volatile elements are negligible. The degree of volatile element depletion correlates with the abundance of accreted chondrules, planetary size, and their accretion timescale. The present-day bulk silicate Earth composition is consistent with a Moon-forming impactor having a Mars-like size and composition. Planetary chemistry, which is related to many factors including the building block composition, the timing, duration and sequence of accretion and its differentiation history, play an essential role in making a planet habitable.

Author contributions

TY and WFM proposed and conceived various portions of this study and together calculated the compositional models of planets. The manuscript was jointly written by TY and WFM and they read and approved the final manuscript.

Competing interests

The authors declare no competing interests.

Additional information

Correspondence and requests for materials should be addressed to TY.

Data and materials availability

Materials used in this study are available within the paper or supplementary materials.

Declaration of Competing Interest

The authors report no declarations of interest.

Acknowledgments

We thank many our colleagues who have listened to various versions of this project and given feedback, especially Eiji Ohtani, Nick Schmerr, Beda Roskovec, Ondřej Šrámek, Sarah Stewart-Mukhopadhyay, Kevin Righter, and Henri Samuel. We also thank Attilio Rivoldini for helpful comments. We greatly appreciate Hugh O'Neill, Bernard Wood, and an anonymous referee for their constructive reviews, which helped improve the manuscript. We thank the journal editor Astrid Holzheid for editorial efforts. TY acknowledges supports from the Japanese Society for the Promotion of Science (JP18J20708) and GP-EES and DIARE research grants. WFM gratefully acknowledges NSF support (EAR1650365).

Appendix A. Supplementary Data

Supplementary data associated with this article can be found, in the online version, at https://doi.org/10.1016/j.chemer.2021.125746.

References

Acuña, M.H., Connerney, J.E., Ness, N.F., Lin, R.P., Mitchell, D., Carlson, C.W., McFadden, J., Anderson, K.A., Rème, H., Mazelle, C., Vignes, D., Wasilewski, P., Cloutier, P., 1999. Global distribution of crustal magnetization discovered by the Mars Global Surveyor MAG/ER experiment. Science 284, 790–793. https://doi.org/10.1126/science.284.5415.790.

Albarede, F., 2009. Volatile accretion history of the terrestrial planets and dynamic implications. Nature 461, 1227–1233. https://doi.org/10.1038/nature08477.

Alexander, C.M.O'D., 2005. Re-examining the role of chondrules in producing the elemental fractionations in chondrites. Meteor. Planet. Sci. 40, 943–965. https://doi.org/10.1111/j. 1945-5100.2005.tb00166.x.

Alexander, C.M.O'D., 2019a. Quantitative models for the elemental and isotopic fractionations in chondrites: The carbonaceous chondrites. Geochim. Cosmochim. Acta 254, 277–309. https://doi.org/10.1016/j.gca.2019.02.008.

Alexander, C.M.O'D., 2019b. Quantitative models for the elemental and isotopic fractionations in the chondrites: The non-carbonaceous chondrites. Geochim. Cosmochim. Acta 254, 246–276. https://doi.org/10.1016/j.gca.2019.01.026.

Alexander, C.M.O'D., Bowden, R., Fogel, M.L., Howard, K.T., Herd, C.D.K., Nittler, L.R., 2012. The provenances of asteroids, and their contributions to the volatile inventories of the terrestrial planets. Science 337, 721–723. https://doi.org/10.1126/science.1223474.

Alexander, C.M.O'D., Grossman, J.N., Ebel, D.S., Ciesla, F.J., 2008. The formation conditions of chondrules and chondrites. Science 320, 1617–1619. https://doi.org/10.1126/science.1156561.

Alexander, C.M.O'D., Grossman, J.N., Wang, J., Zanda, B., Bourot-Denise, M., Hewins, R. H., 2000. The lack of potassium-isotopic fractionation in Bishunpur chondrules. Meteor. Planet. Sci. 35, 859–868. https://doi.org/10.1111/j.1945-5100.2000.tb01469.x.

Allègre, C.J., Poirier, J.P., Humler, E., Hofmann, A.W., 1995. The chemical composition of the Earth. Earth Planet. Sci. Lett. 134, 515–526. https://doi.org/10.1016/0012-821X(95)00123-T.

Amelin, Y., Krot, A., 2007. Pb isotopic age of the Allende chondrules. Meteor. Planet. Sci. 42, 1321–1335. https://doi.org/10.1111/j.1945-5100.2007.tb00577.x.

Amelin, Y., Krot, A.N., Hutcheon, I.D., Ulyanov, A.A., 2002. Lead isotopic ages of chondrules and calcium-aluminum-rich inclusions. Science 297, 1678–1683. https://doi.org/10.1126/science.1073950.

Amsellem, E., Moynier, F., Pringle, E.A., Bouvier, A., Chen, H., Day, J.M.D., 2017. Testing the chondrule-rich accretion model for planetary embryos using calcium isotopes. Earth Planet. Sci. Lett. 469, 75–83. https://doi.org/10.1016/j.epsl.2017.04.022.

Anders, E., Owen, T., 1977. Mars and Earth: Origin and abundance of volatiles. Science 198, 453–465. https://doi.org/10.1126/science.198.4316.453.

Arkani-Hamed, J., 2004. Timing of the Martian core dynamo. J. Geophys. Res.: Planets 109, E03006. https://doi.org/10.1029/2003JE002195.

Ballhaus, C., Fonseca, R.O.C., Münker, C., Rohrbach, A., Nagel, T., Speelmanns, I.M., Helmy, H.M., Zirner, A., Vogel, A.K., Heuser, A., 2017. The great sulfur depletion of Earth's mantle is not a signature of mantle-core equilibration. Contrib. Mineral. Petrol. 172, 68. https://doi.org/10.1007/s00410-017-1388-3.

Ballhaus, C., Laurenz, V., Münker, C., Fonseca, R.O.C., Albarède, F., Rohrbach, A., Lagos, M., Schmidt, M.W., Jochum, K.P., Stoll, B., Weis, U., Helmy, H.M., 2013. The U/Pb ratio of the Earth's mantle—A signature of late volatile addition. Earth Planet. Sci. Lett. 362, 237–245. https://doi.org/10.1016/j.epsl.2012.11.049.

Banerdt, W.B., Smrekar, S.E., Banfield, D., Giardini, D., Golombek, M., Johnson, C.L., Lognonné, P., Spiga, A., Spohn, T., Perrin, C., Stähler, S.C., Antonangeli, D., Asmar, S., Beghein, C., Bowles, N., Bozdag, E., Chi, P., Christensen, U., Clinton, J., Collins, G.S., Daubar, I., Dehant, V., Drilleau, M., Fillingim, M., Folkner, W., Garcia, R.F., Garvin, J., Grant, J., Grott, M., Grygorczuk, J., Hudson, T., Irving, J.C. E., Kargl, G., Kawamura, T., Kedar, S., King, S., Knapmeyer-Endrun, B., Knapmeyer, M., Lemmon, M., Lorenz, R., Maki, J.N., Margerin, L., McLennan, S.M., Michaut, C., Mimoun, D., Mittelholz, A., Mocquet, A., Morgan, P., Mueller, N.T., Murdoch, N., Nagihara, S., Newman, C., Nimmo, F., Panning, M., Pike, W.T., Plesa, A.C., Rodriguez, S., Rodriguez-Manfredi, J.A., Russell, C.T., Schmerr, N., Siegler, M., Stanley, S., Stutzmann, E., Teanby, N., Tromp, J., van Driel, M., Warner, N., Weber, R., Wieczorek, M., 2020. Initial results from the InSight mission on Mars. Nature Geoscience 13, 1–7. https://doi.org/10.1038/s41561-020-0544-y.

Baratoux, D., Toplis, M.J., Monnereau, M., Gasnault, O., 2011. Thermal history of Mars inferred from orbital geochemistry of volcanic provinces. Nature 472, 338–341. https://doi.org/10.1038/nature09903.

Baratoux, D., Toplis, M.J., Monnereau, M., Sautter, V., 2013. The petrological expression of early Mars volcanism. J. Geophys. Res.: Planets 118, 59–64. https://doi.org/10.1029/2012JE004234.

Becker, H., Horan, M.F., Walker, R.J., Gao, S., Lorand, J.P., Rudnick, R.L., 2006. Highly siderophile element composition of the Earth's primitive upper mantle: constraints from new data on peridotite massifs and xenoliths. Geochim. Cosmochim. Acta 70, 4528–4550. https://doi.org/10.1016/j.gca.2006.06.004.

Bermingham, K.R., Gussone, N., Mezger, K., Krause, J., 2018. Origins of mass-dependent and mass-independent Ca isotope variations in meteoritic components and meteorites. Geochim. Cosmochim. Acta 226, 206–223. https://doi.org/10.1016/j.gca.2018.01.034.

Bertka, C.M., Fei, Y., 1997. Mineralogy of the Martian interior up to core-mantle boundary pressures. J. Geophys. Res.: Solid Earth 102, 5251–5264. https://doi.org/10.1029/96JB03270.

Bizzarro, M., Baker, J.A., Haack, H., 2004. Mg isotope evidence for contemporaneous formation of chondrules and refractory inclusions. Nature 431, 275–278. https://doi.org/10.1038/nature02882.

Blanchard, I., Siebert, J., Borensztajn, S., Badro, J., 2017. The solubility of heat-producing elements in Earth's core. Geochem. Perspect. Lett. 5, 1–5. https://doi.org/10.7185/geochemlet.1737.

Bland, P.A., Alard, O., Benedix, G.K., Kearsley, A.T., Menzies, O.N., Watt, L.E., Rogers, N. W., 2005. Volatile fractionation in the early solar system and chondrule/matrix complementarity. Proc. Natl. Acad. Sci. 102, 13755–13760. https://doi.org/10.1073/pnas.0501885102.

van Boekel, R.J.H.M., Min, M., Leinert, C., Waters, L.B.F.M., Richichi, A., Chesneau, O., Dominik, C., Jaffe, W., Dutrey, A., Graser, U., Henning, T., de Jong, J., Köhler, R., de Koter, A., Lopez, B., Malbet, F., Morel, S., Paresce, F., Perrin, G., Preibisch, T., Przygodda, F., Schöller, M., Wittkowski, M., 2004. The building blocks of planets within the 'terrestrial' region of protoplanetary disks. Nature 432, 479–482. https://doi.org/10.1038/nature03088.

Bollard, J., Connelly, J.N., Whitehouse, M.J., Pringle, E.A., Bonal, L., Jørgensen, J.K., Nordlund, Å., Moynier, F., Bizzarro, M., 2017. Early formation of planetary building blocks inferred from Pb isotopic ages of chondrules. Sci. Adv. 3, e1700407. https://doi.org/10.1126/sciadv.1700407.

Bollard, J., Kawasaki, N., Sakamoto, N., Olsen, M., Itoh, S., Larsen, K., Wielandt, D., Schiller, M., Connelly, J.N., Yurimoto, H., Bizzarroa, M., 2019. Combined U-corrected Pb-Pb dating and ^{26}Al-^{26}Mg systematics of individual chondrules-Evidence for a reduced initial abundance of ^{26}Al amongst inner Solar System chondrules. Geochim. Cosmochim. Acta 260, 62–83. https://doi.org/10.1016/j.gca.2019.06.025.

Bouvier, A., Vervoort, J.D., Patchett, P.J., 2008. The Lu-Hf and Sm-Nd isotopic composition of CHUR: Constraints from unequilibrated chondrites and implications for the bulk composition of terrestrial planets. Earth Planet. Sci. Lett. 273, 48–57. https://doi.org/10.1016/j.epsl.2008.06.010.

Bouvier, A., Wadhwa, M., Simon, S.B., Grossman, L., 2013. Magnesium isotopic fractionation in chondrules from the Murchison and Murray CM2 carbonaceous chondrites. Meteor. Planet. Sci. 48, 339–353. https://doi.org/10.1111/maps.12059.

Bouvier, L.C., Costa, M.M., Connelly, J.N., Jensen, N.K., Wielandt, D., Storey, M., Nemchin, A.A., Whitehouse, M.J., Snape, J.F., Bellucci, J.J., Moynier, F., Agranier, A., Gueguen, B., Schönbächler, M., Bizzarro, M., 2018. Evidence for extremely rapid magma ocean crystallization and crust formation on Mars. Nature 558, 586–589. https://doi.org/10.1038/s41586-018-0222-z.

Bouwman, J., Henning, T., Hillenbrand, L.A., Meyer, M.R., Pascucci, I., Carpenter, J., Hines, D., Kim, J.S., Silverstone, M.D., Hollenbach, D., Wolf, S., 2008. The formation and evolution of planetary systems: Grain growth and chemical processing of dust in T Tauri systems. Astrophys. J. 683, 479–498. https://doi.org/10.1086/587793.

Bouwman, J., Lawson, W.A., Juhász, A., Dominik, C., Feigelson, E.D., Henning, T., Tielens, A.G.G.M., Waters, L.B.F.M., 2010. The protoplanetary disk around the M4 star RECX 5: witnessing the influence of planet formation? Astrophys. J. Lett. 5 (723), L243–L247. https://doi.org/10.1088/2041-8205/723/2/L243.

Brandon, A.D., Puchtel, I.S., Walker, R.J., Day, J.M.D., Irving, A.J., Taylor, L.A., 2012. Evolution of the martian mantle inferred from the ^{187}Re-^{187}Os isotope and highly siderophile element abundance systematics of shergottite meteorites. Geochim. Cosmochim. Acta 76, 206–235. https://doi.org/10.1016/j.gca.2011.09.047.

Breuer, D., Moore, W.B., 2015. Dynamics and Thermal History of the Terrestrial Planets, the Moon, and Io. In: Schubert, G. (Ed.), Treatise on Geophysics, 2nd Edition. Elsevier, Oxford, pp. 255–305. https://doi.org/10.1016/B978-0-444-53802-4.00173-1.

Breuer, D., Spohn, T., 2003. Early plate tectonics versus single-plate tectonics on Mars: Evidence from magnetic field history and crust evolution. J. Geophys. Res.: Planets 108, 5072. https://doi.org/10.1029/2002JE001999.

Budde, G., Burkhardt, C., Kleine, T., 2019. Molybdenum isotopic evidence for the late accretion of outer Solar System material to Earth. Nature Astronomy 3, 736–741. https://doi.org/10.1038/s41550-019-0779-y.

Budde, G., Kleine, T., Kruijer, T.S., Burkhardt, C., Metzler, K., 2016. Tungsten isotopic constraints on the age and origin of chondrules. Proceedings of the National Academy of Sciences 113, 2886–2891. https://doi.org/10.1073/pnas.1524980113.

Budde, G., Kruijer, T.S., Kleine, T., 2018. Hf-W chronology of CR chondrites: Implications for the timescales of chondrule formation and the distribution of ^{26}Al in the solar nebula. Geochim. Cosmochim. Acta 222, 284–304. https://doi.org/10.1016/j.gca.2017.10.014.

Burkhardt, C., Borg, L.E., Brennecka, G.A., Shollenberger, Q.R., Dauphas, N., Kleine, T., 2016. A nucleosynthetic origin for the Earth's anomalous ^{142}Nd composition. Nature 537, 394–398. https://doi.org/10.1038/nature18956.

Burkhardt, C., Kleine, T., Oberli, F., Pack, A., Bourdon, B., Wieler, R., 2011. Molybdenum isotope anomalies in meteorites: Constraints on solar nebula evolution and origin of the Earth. Earth Planet. Sci. Lett. 312, 390–400. https://doi.org/10.1016/j.epsl.2011.10.010.

Cano, E.J., Sharp, Z.D., Shearer, C.K., 2020. Distinct oxygen isotope compositions of the Earth and Moon. Nature Geosci. 13, 270–274. https://doi.org/10.1038/s41561-020-0550-0.

Canup, R., Salmon, J., 2018. Origin of phobos and deimos by the impact of a Vesta-to-Ceres sized body with Mars. Sci. Adv. 4, eaar6887. https://doi.org/10.1126/sciadv.aar6887.

Canup, R.M., 2004. Simulations of a late lunar-forming impact. Icarus 168, 433–456. https://doi.org/10.1016/j.icarus.2003.09.028.

Canup, R.M., 2008. Accretion of the Earth. Philos. Trans. Royal Soc. A: Math. Phys. Eng. Sci. 366, 4061–4075. https://doi.org/10.1098/rsta.2008.0101.

Canup, R.M., Asphaug, E., 2001. Origin of the Moon in a giant impact near the end of the Earth's formation. Nature 412, 708–712. https://doi.org/10.1038/35089010.

Caro, G., Bourdon, B., 2010. Non-chondritic Sm/Nd ratio in the terrestrial planets: Consequences for the geochemical evolution of the mantle-crust system. Geochim. Cosmochim. Acta 74, 3333–3349. https://doi.org/10.1016/j.gca.2010.02.025.

Chabot, N.L., 2018. Composition of metallic cores in the early Solar System. Lunar Planet. Sci. Conf. 1532.

Chambat, F., Ricard, Y., Valette, B., 2010. Flattening of the Earth: further from hydrostaticity than previously estimated. Geophys. J. Int. 183, 727–732. https://doi.org/10.1111/j.1365-246X.2010.04771.x.

Cockell, C., Bush, T., Bryce, C., Direito, S., Fox-Powell, M., Harrison, J., Lammer, H., Landenmark, H., Martin-Torres, J., Nicholson, N., Noack, L., O'Malley-James, J., Payler, S., Rushby, A., Samuels, T., Schwendner, P., Wadsworth, J., Zorzano, M., 2016. Habitability: a review. Astrobiology 16, 89–117. https://doi.org/10.1089/ast.2015.1295.

Connelly, J.N., Amelin, Y., Krot, A.N., Bizzarro, M., 2008. Chronology of the solar system's oldest solids. Astrophys. J. Lett. 675, L121–L124. https://doi.org/10.1086/533586.

Connelly, J.N., Bizzarro, M., 2009. Pb-Pb dating of chondrules from CV chondrites by progressive dissolution. Chem. Geol. 259, 143–151. https://doi.org/10.1016/j.chemgeo.2008.11.003.

Connelly, J.N., Bizzarro, M., Krot, A.N., Nordlund, Å., Wielandt, D., Ivanova, M.A., 2012. The absolute chronology and thermal processing of solids in the solar protoplanetary disk. Science 338, 651–655. https://doi.org/10.1126/science.1226919.

Connelly, J.N., Schiller, M., Bizzarro, M., 2019. Pb isotope evidence for rapid accretion and differentiation of planetary embryos. Earth and Planetary Science Letters 525, 115722. https://doi.org/10.1016/j.epsl.2019.115722.

Corgne, A., Keshav, S., Fei, Y., McDonough, W.F., 2007. How much potassium is in the Earth's core? New insights from partitioning experiments. Earth Planet. Sci. Lett. 256, 567–576. https://doi.org/10.1016/j.epsl.2007.02.012.

Creech, J.B., Moynier, F., 2019. Tin and zinc stable isotope characterisation of chondrites and implications for early Solar System evolution. Chem. Geol. 511, 81–90. https://doi.org/10.1016/j.chemgeo.2019.02.028.

Dauphas, N., 2017. The isotopic nature of the Earth's accreting material through time. Nature 541, 521–524. https://doi.org/10.1038/nature20830.

Dauphas, N., Burkhardt, C., Warren, P.H., Fang-Zhen, T., 2014. Geochemical arguments for an Earth-like Moon-forming impactor. Philos. Trans. Royal Soc. A: Math. Phys. Eng. Sci. 372, 20130244. https://doi.org/10.1098/rsta.2013.0244.

Dauphas, N., Poitrasson, F., Burkhardt, C., Kobayashi, H., Kurosawa, K., 2015. Planetary and meteoritic Mg/Si and δ^{30}Si variations inherited from solar nebula chemistry. Earth Planet. Sci. Lett. 427, 236–248. https://doi.org/10.1016/j.epsl.2015.07.008.

Dauphas, N., Pourmand, A., 2011. Hf-W-Th evidence for rapid growth of Mars and its status as a planetary embryo. Nature 473, 489–492. https://doi.org/10.1038/nature10077.

Dauphas, N., Pourmand, A., 2015. Thulium anomalies and rare earth element patterns in meteorites and Earth: Nebular fractionation and the nugget effect. Geochim. Cosmochim. Acta 163, 234–261. https://doi.org/10.1016/j.gca.2015.03.037.

Day, J.M.D., Brandon, A.D., Walker, R.J., 2016. Highly siderophile elements in Earth, Mars, the Moon, and asteroids. Rev. Mineral. Geochem. 81, 161–238. https://doi.org/10.2138/rmg.2016.81.04.

Desch, S.J., Kalyaan, A., Alexander, C.M.O'D, 2018. The effect of Jupiter's formation on the distribution of refractory elements and inclusions in meteorites. Astrophys. J. Suppl. Series 238, 11. https://doi.org/10.3847/1538-4365/aad95f.

Doyle, P.M., Jogo, K., Nagashima, K., Krot, A.N., Wakita, S., Ciesla, F.J., Hutcheon, I.D., 2015. Early aqueous activity on the ordinary and carbonaceous chondrite parent bodies recorded by fayalite. Nature Commun. 6, 7444. https://doi.org/10.1038/ncomms8444.

Dreibus, G., Wänke, H., 1979. On the chemical composition of the Moon and the Eucrite parent body and a comparison with the composition of the Earth, the case of Mn, Cr, and V. Lunar Planet. Sci. Conf. 315–317.

Dreibus, G., Wänke, H., 1987. Volatiles on Earth and Mars: A comparison. Icarus 71, 225–240. https://doi.org/10.1016/0019-1035(87)90148-5.

Dumoulin, C., Tobie, G., Verhoeven, O., Rosenblatt, P., Rambaux, N., 2017. Tidal constraints on the interior of Venus. J. Geophys. Res.: Planets 122, 1338–1352. https://doi.org/10.1002/2016JE005249.

Dziewonski, A.M., Anderson, D.L., 1981. Preliminary reference Earth model. Phys. Earth Planet. Interiors 25, 297–356. https://doi.org/10.1016/0031-9201(81)90046-7.

Ehlmann, B.L., Anderson, F.S., Andrews-Hanna, J., Catling, D.C., Christensen, P.R., Cohen, B.A., Dressing, C.D., Edwards, C.S., Elkins-Tanton, L.T., Farley, K.A., Fassett, C.I., Fischer, W.W., Fraeman, A.A., Golombek, M.P., Hamilton, V.E., Hayes, A.G., Herd, C.D., Horgan, B., Hu, R., Jakosky, B.M., Johnson, J.R., Kasting, J. F., Kerber, L., Kinch, K.M., Kite, E.S., Knutson, H.A., Lunine, J.I., Mahaffy, P.R., Mangold, N., McCubbin, F.M., Mustard, J.F., Niles, P.B., Quantin-Nataf, C., Rice, M. S., Stack, K.M., Stevenson, D.J., Stewart, S.T., Toplis, M.J., Usui, T., Weiss, B.P., Werner, S.C., Wordsworth, R.D., Wray, J.J., Yingst, R.A., Yung, Y.L., Zahnle, K.J., 2016. The sustainability of habitability on terrestrial planets: Insights, questions, and needed measurements from Mars for understanding the evolution of Earth-like worlds. J. Geophys. Res.: Planets 121, 1927–1961. https://doi.org/10.1002/2016JE005134.

Filiberto, J., 2017. Geochemistry of Martian basalts with constraints on magma genesis. Chem. Geol. 466, 1–14. https://doi.org/10.1016/j.chemgeo.2017.06.009.

Filiberto, J., Dasgupta, R., 2011. Fe^{2+}-Mg partitioning between olivine and basaltic melts: Applications to genesis of olivine-phyric shergottites and conditions of melting in the Martian interior. Earth Planet. Sci. Lett. 304, 527–537. https://doi.org/10.1016/j.epsl.2011.02.029.

Frost, D.J., 2003. The structure and sharpness of $(Mg,Fe)_2SiO_4$ phase transformations in the transition zone. Earth Planet. Sci. Lett. 216, 313–328. https://doi.org/10.1016/S0012-821X(03)00533-8.

Fujiya, W., Sugiura, N., Hotta, H., Ichimura, K., Sano, Y., 2012. Evidence for the late formation of hydrous asteroids from young meteoritic carbonates. Nature Commun. 3, 1–6. https://doi.org/10.1038/ncomms1635.

Gaetani, G.A., Grove, T.L., 1999. Wetting of mantle olivine by sulfide melt: implications for Re/Os ratios in mantle peridotite and late-stage core formation. Earth Planet. Sci. Lett. 169, 147–163. https://doi.org/10.1016/S0012-821X(99)00062-X.

Galy, A., Young, E.D., Ash, R.D., O'Nions, R.K., 2000. The formation of chondrules at high gas pressures in the solar nebula. Science 290, 1751–1753. https://doi.org/10.1126/science.290.5497.1751.

Gast, P.W., 1960. Limitations on the composition of the upper mantle. J. Geophys. Res. 65, 1287–1297. https://doi.org/10.1029/JZ065i004p01287.

Gellissen, M., Holzheid, A., Kegler, P., Palme, H., 2019. Heating experiments relevant to the depletion of Na, K and Mn in the Earth and other planetary bodies. Geochemistry 79, 125540. https://doi.org/10.1016/j.chemer.2019.125540.

Genova, A., Goossens, S., Lemoine, F.G., Mazarico, E., Neumann, G.A., Smith, D.E., Zuber, M.T., 2016. Seasonal and static gravity field of Mars from MGS, Mars Odyssey and MRO radio science. Icarus 272, 228–245. https://doi.org/10.1016/j.icarus.2016.02.050.

Goldstein, J.I., Scott, E.R.D., Chabot, N.L., 2009. Iron meteorites: Crystallization, thermal history, parent bodies, and origin. Geochemistry 69, 293–325. https://doi.org/10.1016/j.chemer.2009.01.002.

Goodrich, C.A., Herd, C.D.K., Taylor, L.A., 2003. Spinels and oxygen fugacity in olivine-phyric and lherzolitic shergottites. Meteor. Planet. Sci. 38, 1773–1792. https://doi.org/10.1111/j.1945-5100.2003.tb00014.x.

Greenwood, R.C., Barrat, J.A., Miller, M.F., Anand, M., Dauphas, N., Franchi, I.A., Sillard, P., Starkey, N.A., 2018. Oxygen isotopic evidence for accretion of Earth's water before a high-energy Moon-forming giant impact. Sci. Adv. 4, eaao5928. https://doi.org/10.1126/sciadv.aao5928.

Grossman, L., Ebel, D.S., Simon, S.B., Davis, A.M., Richter, F.M., Parsad, N.M., 2000. Major element chemical and isotopic compositions of refractory inclusions in C3 chondrites: The separate roles of condensation and evaporation. Geochim. Cosmochim. Acta 64, 2879–2894. https://doi.org/10.1016/S0016-7037(00)00396-3.

Grossman, L., Simon, S.B., Rai, V.K., Thiemens, M.H., Hutcheon, I.D., Williams, R.W., Galy, A., Ding, T., Fedkin, A.V., Clayton, R.N., Mayeda, T.K., 2008. Primordial compositions of refractory inclusions. Geochim. Cosmochim. Acta 72, 3001–3021. https://doi.org/10.1016/j.gca.2008.04.002.

Halliday, A.N., Porcelli, D., 2001. In search of lost planets-The paleocosmochemistry of the inner solar system. Earth Planet. Sci. Lett. 192, 545–559. https://doi.org/10.1016/S0012-821X(01)00479-4.

Hans, U., Kleine, T., Bourdon, B., 2013. Rb-Sr chronology of volatile depletion in differentiated protoplanets: BABI, ADOR and ALL revisited. Earth Planet. Sci. Lett. 374, 204–214. https://doi.org/10.1016/j.epsl.2013.05.029.

Harrison, J.H., Shorttle, O., Bonsor, A., 2021. Evidence for post-nebula volatilisation in an exo-planetary body. Earth Planet. Sci. Lett. 554, 116694. https://doi.org/10.1016/j.epsl.2020.116694.

Harrison, J.H.D., Bonsor, A., Madhusudhan, N., 2018. Polluted white dwarfs: constraints on the origin and geology of exoplanetary material. Monthly Notices Royal Astron. Soc. 479, 3814–3841. https://doi.org/10.1093/mnras/sty1700.

Hart, S.R., Zindler, A., 1986. In search of a bulk-Earth composition. Chem. Geol. 57, 247–267. https://doi.org/10.1016/0009-2541(86)90053-7.

Herd, C.D.K., 2019. Reconciling redox: making spatial and temporal sense of oxygen fugacity variations in martian igneous rocks. Lunar Planet. Sci. Conf. 2746.

Herd, C.D.K., Borg, L.E., Jones, J.H., Papike, J.J., 2002. Oxygen fugacity and geochemical variations in the martian basalts: Implications for martian basalt petrogenesis and the oxidation state of the upper mantle of Mars. Geochim. Cosmochim. Acta 66, 2025–2036. https://doi.org/10.1016/S0016-7037(02)00828-1.

Herd, C.D.K., Papike, J.J., Brearley, A.J., 2001. Oxygen fugacity of martian basalts from electron microprobe oxygen and TEM-EELS analyses of Fe-Ti oxides. Am. Mineral. 86, 1015–1024. https://doi.org/10.2138/am-2001-8-908.

Hewins, R.H., Herzberg, C.T., 1996. Nebular turbulence, chondrule formation, and the composition of the Earth. Earth Planet. Sci. Lett. 144, 1–7. https://doi.org/10.1016/0012-821X(96)00159-8.

Hewins, R.H., Zanda, B., 2012. Chondrules: Precursors and interactions with the nebular gas. Meteor. Planet. Sci. 47, 1120–1138. https://doi.org/10.1111/j. 1945-5100.2012.01376.x.

Hezel, D.C., Bland, P., Palme, H., Jacquet, E., Bigolski, J., 2018a. Composition of chondrules and matrix and their complementary relationship in chondrites. In: Russell, S.S., Connolly, H.C.JJr., Krot, A.N. (Eds.), Chondrules and the Protoplanetary Disk. Cambridge University Press, Cambridge, pp. 91–121 chapter 4, doi: 10.1017/9781108284073.004.

Hezel, D.C., Harak, M., Libourel, G., 2018b. What we know about elemental bulk chondrule and matrix compositions: Presenting the ChondriteDB Database. Chemie der Erde-Geochemistry 78, 1–14. https://doi.org/10.1016/j.chemer.2017.05.003.

Hin, R.C., Coath, C.D., Carter, P.J., Nimmo, F., Lai, Y.J., von Strandmann, P.A.E.P., Willbold, M., Leinhardt, Z.M., Walter, M.J., Elliott, T., 2017. Magnesium isotope evidence that accretional vapour loss shapes planetary compositions. Nature 549, 511–515. https://doi.org/10.1038/nature23899.

Hosono, N., Karato, S., Makino, i., Saitoh, J., 2019. Terrestrial magma ocean origin of the Moon. Nature Geosci. 12, 418–423. https://doi.org/10.1038/s41561-019-0354-2.

Huang, S., Farkaš, J., Jacobsen, S.B., 2010. Calcium isotopic fractionation between clinopyroxene and orthopyroxene from mantle peridotites. Earth Planet. Sci. Lett. 292, 337–344. https://doi.org/10.1016/j.epsl.2010.01.042.

Humayun, M., Clayton, R.N., 1995. Potassium isotope cosmochemistry: Genetic implications of volatile element depletion. Geochim. Cosmochim. Acta 59, 2131–2148. https://doi.org/10.1016/0016-7037(95)00132-8.

Humayun, M., Nemchin, A., Zanda, B., Hewins, R.H., Grange, M., Kennedy, A., Lorand, J. P., Göpel, C., Fieni, C., Pont, S., Deldicque, D., 2013. Origin and age of the earliest Martian crust from meteorite NWA 7533. Nature 503, 513–516. https://doi.org/10.1038/nature12764.

Jackson, A.P., Gabriel, T.S.J., Asphaug, E.I., 2018. Constraints on the pre-impact orbits of Solar system giant impactors. Monthly Notices Royal Astron. Soc. 474, 2924–2936. https://doi.org/10.1093/mnras/stx2901.

Jagoutz, E., Palme, H., Baddenhausen, H., Blum, K., Cendales, M., Dreibus, G., Spettel, B., Lorenz, V., Wänke, H., 1979. The abundances of major, minor and trace elements in the earth's mantle as derived from primitive ultramafic nodules. Lunar Planet. Sci. Conf/ Proc. 2031–2050.

Jaupart, C., Labrosse, S., Lucazeau, F., Mareschal, J.C., 2015. Temperatures, heat, and energy in the mantle of the earth. In: Schubert, G. (Ed.), Treatise on Geophysics, 2nd Edition. Elsevier, Oxford, pp. 223–270. volume 7, doi: 10.1016/B978-0-444-53802-4.00126-3.

Javoy, M., 1995. The integral enstatite chondrite model of the Earth. Geophys. Res. Lett. 22, 2219–2222. https://doi.org/10.1029/95GL02015.

Javoy, M., Kaminski, E., Guyot, F., Andrault, D., Sanloup, C., Moreira, M., Labrosse, S., Jambon, A., Agrinier, P., Davaille, A., Jaupart, C., 2010. The chemical composition of the Earth: Enstatite chondrite models. Earth Planet. Sci. Lett. 293, 259–268. https://doi.org/10.1016/j.epsl.2010.02.033.

Johansen, A., Jacquet, E., Cuzzi, J.N., Morbidelli, A., Gounelle, M., 2015a. New paradigms for asteroid formation. In: Michel, P., DeMeo, F., Bottke, W., Dotson, R. (Eds.), Asteroids IV. University of Arizona Press, Tucson, pp. 471–492 volume 47, doi: 10.2458/azu_uapress_9780816532131-ch025.

Johansen, A., Mac Low, M.M., Lacerda, P., Bizzarro, M., 2015b. Growth of asteroids, planetary embryos, and Kuiper belt objects by chondrule accretion. Sci. Adv. 1, e1500109. https://doi.org/10.1126/sciadv.1500109.

Johnson, B.C., Minton, D.A., Melosh, H.J., Zuber, M.T., 2015. Impact jetting as the origin of chondrules. Nature 517, 339–341. https://doi.org/10.1038/nature14105.

Jones, R.H., 1994. Relict grains in chondrules: Evidence for chondrule recycling. In: Hewins, R.H., Jones, R.H., Scott, E.R.D. (Eds.), Chondrules and the Protoplanetary Disk, pp. 163–172.

Kato, C., Moynier, F., 2017. Gallium isotopic evidence for extensive volatile loss from the Moon during its formation. Sci. Adv. 3, e1700571. https://doi.org/10.1126/sciadv.1700571.

Katsura, T., Yoneda, A., Yamazaki, D., Yoshino, T., Ito, E., 2010. Adiabatic temperature profile in the mantle. Phys. Earth Planet. Interiors 183, 212–218. https://doi.org/10.1016/j.pepi.2010.07.001.

Kerridge, J., 1979. Fractionation of refractory lithophile elements among chondritic meteorites. Lunar Planet. Sci. Conf. Proc. 989–996.

Kessler-Silacci, J., Augereau, J., Dullemond, C.P., Geers, V., Lahuis, F., Evans, I.I., van Dishoeck, N.J., Blake, E.F., Boogert, G.A., Brown, A.C.A., Jorgensen, J., Knez, J.K., Pontoppidan, C.K.M., 2006. C2D Spitzer IRS spectra of disks around T Tauri stars. I. Silicate emission and grain growth. Astrophys. J. 639, 275. https://doi.org/10.1086/499330.

Khan, A., Liebske, C., Rozel, A., Rivoldini, A., Nimmo, F., Connolly, J.A.D., Plesa, A.C., Giardini, D., 2018. A geophysical perspective on the bulk composition of Mars. J. Geophys. Res.: Planets 123, 575–611. https://doi.org/10.1002/2017JE005371.

Kiefer, W.S., 2003. Melting in the Martian mantle: Shergottite formation and implications for present-day mantle convection on Mars. Meteor. Planet. Sci. 38, 1815–1832. https://doi.org/10.1111/j.1945-5100.2003.tb00017.x.

Kimura, K., Lewis, R.S., Anders, E., 1974. Distribution of gold and rhenium between nickel-iron and silicate melts: implications for the abundance of siderophile elements on the Earth and Moon. Geochim. Cosmochim. Acta 38, 683–701. https://doi.org/10.1016/0016-7037(74)90144-6.

Kita, N.T., Yin, Q.Z., MacPherson, G.J., Ushikubo, T., Jacobsen, B., Nagashima, K., Kurahashi, E., Krot, A.N., Jacobsen, S.B., 2013. ^{26}Al-^{26}Mg isotope systematics of the first solids in the early solar system. Meteor. Planet. Sci. 48, 1383–1400. https://doi.org/10.1111/maps.12141.

Kleine, T., Touboul, M., Bourdon, B., Nimmo, F., Mezger, K., Palme, H., Jacobsen, S.B., Yin, Q.Z., Halliday, A.N., 2009. Hf-W chronology of the accretion and early evolution of asteroids and terrestrial planets. Geochim. Cosmochim. Acta 73, 5150–5188. https://doi.org/10.1016/j.gca.2008.11.047.

Konopliv, A.S., Park, R.S., Folkner, W.M., 2016. An improved JPL Mars gravity field and orientation from Mars orbiter and lander tracking data. Icarus 274, 253–260. https://doi.org/10.1016/j.icarus.2016.02.052.

Krot, A.N., Wasson, J.T., 1995. Igneous rims on low-FeO and high-FeO chondrules in ordinary chondrites. Geochim. Cosmochim. Acta 59, 4951–4966. https://doi.org/10.1016/0016-7037(95)00337-1.

Kruijer, T.S., Burkhardt, C., Budde, G., Kleine, T., 2017a. Age of Jupiter inferred from the distinct genetics and formation times of meteorites. Proc. Natl. Acad. Sci. 114, 6712–6716. https://doi.org/10.1073/pnas.1704461114.

Kruijer, T.S., Kleine, T., Borg, L.E., 2020. The great isotopic dichotomy of the early Solar System. Nature Astron. 4, 32–40. https://doi.org/10.1038/s41550-019-0959-9.

Kruijer, T.S., Kleine, T., Borg, L.E., Brennecka, G.A., Irving, A.J., Bischoff, A., Agee, C.B., 2017b. The early differentiation of Mars inferred from Hf-W chronometry. Earth Planet. Sci. Lett. 474, 345–354. https://doi.org/10.1016/j.epsl.2017.06.047.

Larimer, J.W., 1967. Chemical fractionations in meteorites-I. Condensation of the elements. Geochim. Cosmochim. Acta 31, 1215–1238. https://doi.org/10.1016/S0016-7037(67)80013-9.

Larimer, J.W., 1979. The condensation and fractionation of refractory lithophile elements. Icarus 40, 446–454. https://doi.org/10.1016/0019-1035(79)90038-1.

Larimer, J.W., Anders, E., 1967. Chemical fractionations in meteorites-II. Abundance patterns and their interpretation. Geochim. Cosmochim. Acta 31, 1239–1270. https://doi.org/10.1016/S0016-7037(67)80014-0.

Laurenz, V., Rubie, D.C., Frost, D.J., Vogel, A.K., 2016. The importance of sulfur for the behavior of highly-siderophile elements during Earth's differentiation. Geochim. Cosmochim. Acta 194, 123–138. https://doi.org/10.1016/j.gca.2016.08.012.

Levison, H.F., Kretke, K.A., Walsh, K.J., Bottke, W.F., 2015. Growing the terrestrial planets from the gradual accumulation of submeter-sized objects. Proc. Natl. Acad. Sci. 112, 14180–14185. https://doi.org/10.1073/pnas.1513364112.

Li, Y., Dasgupta, R., Tsuno, K., Monteleone, B., Shimizu, N., 2016. Carbon and sulfur budget of the silicate Earth explained by accretion of differentiated planetary embryos. Nature Geosci. 9, 781–785. https://doi.org/10.1038/ngeo2801.

Lillis, R.J., Frey, H.V., Manga, M., 2008. Rapid decrease in Martian crustal magnetization in the Noachian era: Implications for the dynamo and climate of early Mars. Geophys. Res. Lett. 35, L14203. https://doi.org/10.1029/2008GL034338.

Lock, S.J., Stewart, S.T., Petaev, M.I., Leinhardt, Z., Mace, M.T., Jacobsen, S.B., Cuk, M., 2018. The origin of the Moon within a terrestrial synestia. J. Geophys. Res.: Planets 123, 910–951. https://doi.org/10.1002/2017JE005333.

Lodders, K., 2003. Solar system abundances and condensation temperatures of the elements. Astrophys. J. 591, 1220–1247. https://doi.org/10.1086/375492.

Lodders, K., 2020. Solar Elemental Abundances. In: Read, P. (Ed.), Oxford Research Encyclopedia of Planetary Science. Oxford University Press, Oxford, pp. 1–68. https://doi.org/10.1093/acrefore/9780190647926.013.145.

Longhi, J., Knittle, E., Holloway, J.R., Wänke, H., 1992. The bulk composition, mineralogy and internal structure of Mars. In: Kieffer, H.H., Jakosky, B.M., Snyder, C.W., Matthews, M.S. (Eds.), Mars. University of Arizona Press, Tuscon, pp. 184–208.

Lorand, J.P., Conquéré, F., 1983. Contribution à l'étude des sulfures dans les enclaves de lherzolite à spinelle des basaltes alcalins (Massif Central et Languedoc, France). Bull. Minéralogie 106, 585–606. https://doi.org/10.3406/bulmi.1983.7737.

Magna, T., Gussone, N., Mezger, K., 2015. The calcium isotope systematics of Mars. Earth Planet. Sci. Lett. 430, 86–94. https://doi.org/10.1016/j.epsl.2015.08.016.

Mahan, B., Moynier, F., Siebert, J., Gueguen, B., Agranier, A., Pringle, E.A., Bollard, J., Connelly, J.N., Bizzarro, M., 2018. Volatile element evolution of chondrules through time. Proc. Natl. Acad. Sci. 115, 8547–8552. https://doi.org/10.1073/pnas.1807263115.

Maltese, A., Mezger, K., 2020. The Pb isotope evolution of Bulk Silicate Earth: Constraints from its accretion and early differentiation history. Geochim. Cosmochim. Acta 271, 179–193. https://doi.org/10.1016/j.gca.2019.12.021.

Marchi, S., Walker, R.J., Canup, R.M., 2020. A compositionally heterogeneous martian mantle due to late accretion. Sci. Adv. 6, eaay2338. https://doi.org/10.1126/sciadv.aay2338.

Marinova, M.M., Aharonson, O., Asphaug, E., 2008. Mega-impact formation of the Mars hemispheric dichotomy. Nature 453, 1216–1219. https://doi.org/10.1038/nature07070.

Marty, B., 2012. The origins and concentrations of water, carbon, nitrogen and noble gases on Earth. Earth Planet. Sci. Lett. 313, 56–66. https://doi.org/10.1016/j.epsl.2011.10.040.

McCanta, M.C., Elkins-Tanton, L., Rutherford, M.J., 2009. Expanding the application of the Eu-oxybarometer to the lherzolitic shergottites and nakhlites: Implications for the oxidation state heterogeneity of the Martian interior. Meteor. Planet. Sci. 44, 725–745. https://doi.org/10.1111/j.1945-5100.2009.tb00765.x.

McDonough, W.F., 2014. Compositional model for the Earth's core. In: Holland, H.D., Turekian, K.K. (Eds.), Treatise on Geochemistry, 2nd ed. Elsevier, Oxford, pp. 559–577. volume 3, doi: 10.1016/B978-0-08-095975-7.00215-1.

McDonough, W.F., 2016. The composition of the lower mantle and core. In: Terasaki, H., Fischer, R.A. (Eds.), Deep Earth. American Geophysical Union (AGU), pp. 145–159 chapter 12, doi: 10.1002/9781118992487.ch12.

McDonough, W.F., Sun, S.s., 1995. The composition of the Earth. Chem. Geol. 120, 223–253. https://doi.org/10.1016/0009-2541(94)00140-4.

McDonough, W.F., Sun, S., Ringwood, s., Jagoutz, A.E., Hofmann, E.A.W., 1992. Potassium, rubidium, and cesium in the Earth and Moon and the evolution of the mantle of the Earth. Geochim. Cosmochim. Acta 56, 1001–1012. https://doi.org/10.1016/0016-7037(92)90043-I.

McGovern, P.J., Solomon, S.C., Smith, D.E., Zuber, M.T., Simons, M., Wieczorek, M.A., Phillips, R.J., Neumann, G.A., Aharonson, O., Head, J.W., 2002. Localized gravity/topography admittance and correlation spectra on Mars: Implications for regional and global evolution. J. Geophys. Res.: Planets 107, 19-1-19-25. doi: 10.1029/2002JE02002,01854.

McKenzie, D., Barnett, D.N., Yuan, D.N., 2002. The relationship between Martian gravity and topography. Earth Planet. Sci. Lett. 195, 1–16. https://doi.org/10.1016/S0012-821X(01)00555-6.

McSween Jr., H.Y., 1977a. Carbonaceous chondrites of the Ornans type: A metamorphic sequence. Geochim. Cosmochim. Acta 41, 477–491. https://doi.org/10.1016/0016-7037(77)90286-1.

McSween Jr., H.Y., 1977b. Petrographic variations among carbonaceous chondrites of the Vigarano type. Geochim. Cosmochim. Acta 41, 1777–1790. https://doi.org/10.1016/0016-7037(77)90210-1.

McSween Jr., H.Y., 1979. Alteration in CM carbonaceous chondrites inferred from modal and chemical variations in matrix. Geochim. Cosmochim. Acta 43, 1761–1770. https://doi.org/10.1016/0016-7037(79)90024-3.

MetBase, 1994-2017. Meteorite Information Database, URL: http://www.metbase.org. geoPlatform UG, Germany. Accessed: 2019-11-3.

Morbidelli, A., Libourel, G., Palme, H., Jacobson, S.A., Rubie, D.C., 2020. Subsolar Al/Si and Mg/Si ratios of non-carbonaceous chondrites reveal planetesimal formation during early condensation in the protoplanetary disk. Earth Planet. Sci. Lett. 538, 116220. https://doi.org/10.1016/j.epsl.2020.116220.

Morbidelli, A., Lunine, J.I., O'Brien, D.P., Raymond, S.N., Walsh, K.J., 2012. Building terrestrial planets. Annu. Rev. Earth Planet. Sci. 40, 251–275. https://doi.org/10.1146/annurev-earth-042711-105319.

Morgan, J.W., Anders, E., 1980. Chemical composition of Earth, Venus, and Mercury. Proc. Natl. Acad. Sci. 77, 6973–6977. https://doi.org/10.1073/pnas.77.12.6973.

Morris, M.A., Boley, A.C., Desch, S.J., Athanassiadou, T., 2012. Chondrule formation in bow shocks around eccentric planetary embryos. Astrophys. J. 752, 27. https://doi.org/10.1088/0004-637X/752/1/27.

Moynier, F., Day, J.M.D., Okui, W., Yokoyama, T., Bouvier, A., Walker, R.J., Podosek, F.A., 2012. Planetary-scale strontium isotopic heterogeneity and the age of volatile depletion of early Solar System materials. Astrophys. J. 758, 45. https://doi.org/10.1088/0004-637X/758/1/45.

Mukhopadhyay, S., 2012. Early differentiation and volatile accretion recorded in deep-mantle neon and xenon. Nature 486, 101–104. https://doi.org/10.1038/nature11141.

Nagashima, K., Krot, A.N., Komatsu, M., 2017. ^{26}Al-^{26}Mg systematics in chondrules from Kaba and Yamato 980145 CV3 carbonaceous chondrites. Geochim. Cosmochim. Acta 201, 303–319. https://doi.org/10.1016/j.gca.2016.10.030.

Nebel, O., Mezger, K., van Westrenen, W., 2011. Rubidium isotopes in primitive chondrites: Constraints on Earth's volatile element depletion and lead isotope evolution. Earth Planet. Sci. Lett. 305, 309–316. https://doi.org/10.1016/j.gca.2010.04.061.

Norris, C.A., Wood, B.J., 2017. Earth's volatile contents established by melting and vaporization. Nature 549, 507–510. https://doi.org/10.1038/nature23645.

Ohtani, E., Ringwood, A.E., 1984. Composition of the core, I. Solubility of oxygen in molten iron at high temperatures. Earth Planet. Sci. Lett. 71, 85–93. https://doi.org/10.1016/0012-821X(84)90054-2.

Olsen, M.B., Wielandt, D., Schiller, M., Van Kooten, E.M.M.E., Bizzarro, M., 2016. Magnesium and ^{54}Cr isotope compositions of carbonaceous chondrite chondrules-Insights into early disk processes. Geochim. Cosmochim. Acta 191, 118–138. https://doi.org/10.1016/j.gca.2016.07.011.

O'Neill, H.S.C., 1991. The origin of the Moon and the early history of the Earth-A chemical model. Part 1: The Moon. Geochim. Cosmochim. Acta 55, 1135–1157. https://doi.org/10.1016/0016-7037(91)90168-5.

O'Neill, H.S.C., 1991a. The origin of the Moon and the early history of the Earth-A chemical model. Part 2: The Earth. Geochim. Cosmochim. Acta 55, 1159–1172. https://doi.org/10.1016/0016-7037(91)90169-6.

O'Neill, H.S.C., Canil, D., Rubie, D.C., 1998. Oxide-metal equilibria to 2500 °C and 25 GPa: Implications for core formation and the light component in the Earth's core. J. Geophys. Res.: Solid Earth 103, 12239–12260. https://doi.org/10.1029/97JB02601.

O'Neill, H.S.C., Palme, H., 2008. Collisional erosion and the non-chondritic composition of the terrestrial planets. Philos. Trans. Royal Soc. London A: Math. Phys. Eng. Sci. 366, 4205–4238. https://doi.org/10.1098/rsta.2008.0111.

O'Rourke, J.G., Shim, S.H., 2019. Hydrogenation of the Martian core by hydrated mantle minerals with implications for the early dynamo. J. Geophys. Res.: Planets 124, 3422–3441. https://doi.org/10.1029/2019JE005950.

Palme, H., O'Neill, H.S.C., 2014. Cosmochemical estimates of mantle composition. In: Holland, H.D., Turekian, K.K. (Eds.), Treatise on Geochemistry, 2nd Edition. Elsevier, Oxford, pp. 1–39. volume 3, doi: 10.1016/B978-0-08-095975-7.00201-1.

Paniello, R.C., Day, J.M.D., Moynier, F., 2012a. Zinc isotopic evidence for the origin of the Moon. Nature 490, 376–379. https://doi.org/10.1038/nature11507.
Paniello, R.C., Moynier, F., Beck, P., Barrat, J.A., Podosek, F.A., Pichat, S., 2012b. Zinc isotopes in HEDs: Clues to the formation of 4-Vesta, and the unique composition of Pecora Escarpment 82502. Geochim. Cosmochim. Acta 86, 76–87. https://doi.org/10.1016/j.gca.2012.01.045.
Pape, J., Mezger, K., Bouvier, A.S., Baumgartner, L.P., 2019. Time and duration of chondrule formation: Constraints from ^{26}Al-^{26}Mg ages of individual chondrules. Geochim. Cosmochim. Acta 244, 416–436. https://doi.org/10.1016/j.gca.2018.10.017.
Parro, L.M., Jiménez-Díaz, A., Mansilla, F., Ruiz, J., 2017. Present-day heat flow model of Mars. Sci. Reports 7, 45629. https://doi.org/10.1038/srep45629.
Peplowski, P.N., Evans, L.G., Hauck, S.A., McCoy, T.J., Boynton, W.V., Gillis-Davis, J.J., Ebel, D.S., Goldsten, J.O., Hamara, D.K., Lawrence, D.J., McNutt, R.L., Nittler, L.R., Solomon, S.C., Rhodes, E.A., Sprague, A.L., Starr, R.D., Stockstill-Cahill, K.R., 2011. Radioactive elements on Mercury's surface from MESSENGER: Implications for the planet's formation and evolution. Science 333, 1850–1852. https://doi.org/10.1126/science.1211576.
Pilipp, W., Hartquist, T.W., Morfill, G.E., Levy, E., 1998. Chondrule formation by lightning in the Protosolar Nebula? Astron. Astrophys. 331, 121–146.
Poitrasson, F., Halliday, A.N., Lee, D.C., Levasseur, S., Teutsch, N., 2004. Iron isotope differences between Earth, Moon, Mars and Vesta as possible records of contrasted accretion mechanisms. Earth Planet. Sci. Lett. 223, 253–266. https://doi.org/10.1016/j.epsl.2004.04.032.
Poole, G.M., Rehkämper, M., Coles, B.J., Goldberg, T., Smith, C.L., 2017. Nucleosynthetic molybdenum isotope anomalies in iron meteorites-new evidence for thermal processing of solar nebula material. Earth Planet. Sci. Lett. 473, 215–226. https://doi.org/10.1016/j.epsl.2017.05.001.
Prettyman, T.H., Yamashita, N., Reedy, R.C., McSween Jr., H.Y., Mittlefehldt, D.W., Hendricks, J.S., Toplis, M.J., 2015. Concentrations of potassium and thorium within Vesta's regolith. Icarus 259, 39–52. https://doi.org/10.1016/j.icarus.2015.05.035.
Pringle, E.A., Moynier, F., 2017. Rubidium isotopic composition of the Earth, meteorites, and the Moon: Evidence for the origin of volatile loss during planetary accretion. Earth Planet. Sci. Lett. 473, 62–70. https://doi.org/10.1016/j.epsl.2017.05.033.
Pringle, E.A., Moynier, F., Beck, P., Paniello, R., Hezel, D.C., 2017. The origin of volatile element depletion in early solar system material: Clues from Zn isotopes in chondrules. Earth Planet. Sci. Lett. 468, 62–71. https://doi.org/10.1016/j.epsl.2017.04.002.
Pringle, E.A., Moynier, F., Savage, P.S., Badro, J., Barrat, J.A., 2014. Silicon isotopes in angrites and volatile loss in planetesimals. Proc. Natl. Acad. Sci. 111, 17029–17032. https://doi.org/10.1073/pnas.1418889111.
Putirka, K., 2016. Rates and styles of planetary cooling on Earth, Moon, Mars, and Vesta, using new models for oxygen fugacity, ferric-ferrous ratios, olivine-liquid Fe-Mg exchange, and mantle potential temperature. Am. Mineral. 101, 819–840. https://doi.org/10.2138/am-2016-5402.
Raymond, S.N., Quinn, T., Lunine, J.I., 2006. High-resolution simulations of the final assembly of Earth-like planets I. Terrestrial accretion and dynamics. Icarus 183, 265–282. https://doi.org/10.1016/j.icarus.2006.03.011.
Richter, F.M., Davis, A.M., Ebel, D.S., Hashimoto, A., 2002. Elemental and isotopic fractionation of Type B calcium-, aluminum-rich inclusions: Experiments, theoretical considerations, and constraints on their thermal evolution. Geochim. Cosmochim. Acta 66, 521–540. https://doi.org/10.1016/S0016-7037(01)00782-7.
Righter, K., 2019. Volatile element depletion of the Moon-The roles of precursors, post-impact disk dynamics, and core formation. Sci. Adv. 5, eaau7658. https://doi.org/10.1126/sciadv.aau7658.
Righter, K., Chabot, N.L., 2011. Moderately and slightly siderophile element constraints on the depth and extent of melting in early Mars. Meteor. Planet. Sci. 46, 157–176. https://doi.org/10.1111/j.1945-5100.2010.01140.x.
Righter, K., Danielson, L.R., Pando, K.M., Williams, J., Humayun, M., Hervig, R.L., Sharp, T.G., 2015. Highly siderophile element (HSE) abundances in the mantle of Mars are due to core formation at high pressure and temperature. Meteor. Planet. Sci. 50, 604–631. https://doi.org/10.1111/maps.12393.
Righter, K., Humayun, M., Danielson, L., 2008. Partitioning of palladium at high pressures and temperatures during core formation. Nature Geosci. 1, 321–323. https://doi.org/10.1038/ngeo180.
Righter, K., Pando, K., Humayun, M., Waeselmann, N., Yang, S., Boujibar, A., Danielson, L.R., 2018. Effect of silicon on activity coefficients of siderophile elements (Au, Pd, Pt, P, Ga, Cu, Zn, and Pb) in liquid Fe: Roles of core formation, late sulfide matte, and late veneer in shaping terrestrial mantle geochemistry. Geochim. Cosmochim. Acta 232, 101–123. https://doi.org/10.1016/j.gca.2018.04.011.
Righter, K., Pando, K., Ross, D.K., Righter, M., Lapen, T.J., 2019. Effect of silicon on activity coefficients of Bi, Cd, Sn, and Ag in liquid Fe-Si, and implications for differentiation and core formation. Meteor. Planet. Sci. 54, 1379–1394. https://doi.org/10.1111/maps.13285.
Righter, K., Sutton, S.R., Danielson, L., Pando, K., Newville, M., 2016. Redox variations in the inner solar system with new constraints from vanadium XANES in spinels. Am. Mineral. 101, 1928–1942. https://doi.org/10.2138/am-2016-5638.
Ringwood, A.E., 1966. Chemical evolution of the terrestrial planets. Geochim. Cosmochim. Acta 30, 41–104. https://doi.org/10.1016/0016-7037(66)90090-1.
Ringwood, A.E., 1975. Composition and Petrology of the Earth's Mantle. MacGraw-Hill, New York.
Rivoldini, A., Van Hoolst, T., Verhoeven, O., Mocquet, A., Dehant, V., 2011. Geodesy constraints on the interior structure and composition of Mars. Icarus 213, 451–472. https://doi.org/10.1016/j.icarus.2011.03.024.
Rose, L.A., Brenan, J.M., 2001. Wetting properties of Fe-Ni-Co-Cu-Os melts against olivine: Implications for sulfide melt mobility. Econ. Geol. 96, 145–157. https://doi.org/10.2113/gsecongeo.96.1.145.
Rubie, D.C., Frost, D.J., Mann, U., Asahara, Y., Nimmo, F., Tsuno, K., Kegler, P., Holzheid, A., Palme, H., 2011. Heterogeneous accretion, composition and core-mantle differentiation of the Earth. Earth Planet. Sci. Lett. 301, 31–42. https://doi.org/10.1016/j.epsl.2010.11.030.
Rubie, D.C., Jacobson, S.A., Morbidelli, A., O'Brien, D.P., Young, E.D., de Vries, J., Nimmo, F., Palme, H., Frost, D.J., 2015. Accretion and differentiation of the terrestrial planets with implications for the compositions of early-formed Solar System bodies and accretion of water. Icarus 248, 89–108. https://doi.org/10.1016/j.icarus.2014.10.015.
Rubie, D.C., Laurenz, V., Jacobson, S.A., Morbidelli, A., Palme, H., Vogel, A.K., Frost, D.J., 2016. Highly siderophile elements were stripped from Earth's mantle by iron sulfide segregation. Science 353, 1141–1144. https://doi.org/10.1126/science.aaf6919.
Rudnick, R.L., Gao, S., 2014. Composition of the continental crust. In: Holland, H.D., Turekian, K.K. (Eds.), Treatise on Geochemistry, 2nd Edition. Elsevier, Oxford, pp. 1–51. https://doi.org/10.1016/B978-0-08-095975-7.00301-6.
Russell, S.S., Connolly, H.C.JJr., Krot, A.N. (Eds.), 2018. Chondrules: Records of Protoplanetary Disk Processes. volume 22. Cambridge University Press, Cambridge. https://doi.org/10.1017/9781108284073.
Sanders, I.S., Scott, E.R.D., 2018. Making Chondrules by Splashing Molten Planetesimals. In: Russell, S.S., Connolly, H.C.JJr., Krot, A.N. (Eds.), Chondrules: Records of Protoplanetary Disk Processes. Cambridge University Press Cambridge Planetary Science, pp. 361–374 chapter 14, doi: . doi: 10.1017/9781108284073 .014.
Sargent, B.A., Forrest, W.J., Tayrien, C., McClure, M.K., Li, A., Basu, A.R., Manoj, P., Watson, D.M., Bohac, C.J., Furlan, E., Kim, K.H., Green, J.D., Sloan, G.C., 2008. Silica in protoplanetary disks. Astrophys. J. 690, 1193. https://doi.org/10.1088/0004-637X/690/2/1193.
Schiller, M., Bizzarro, M., Fernandes, V.A., 2018. Isotopic evolution of the protoplanetary disk and the building blocks of Earth and the Moon. Nature 555, 507–510. https://doi.org/10.1038/nature25990.
Schönbächler, M., Carlson, R.W., Horan, M.F., Mock, T.D., Hauri, E.H., 2010. Heterogeneous accretion and the moderately volatile element budget of Earth. Science 328, 884–887. https://doi.org/10.1126/science.1186239.
Schrader, D.L., Nagashima, K., Krot, A.N., Ogliore, R.C., Yin, Q.Z., Amelin, Y., Stirling, C.H., Kaltenbach, A., 2017. Distribution of ^{26}Al in the CR chondrite chondrule-forming region of the protoplanetary disk. Geochim. Cosmochim. Acta 201, 275–302. https://doi.org/10.1016/j.gca.2016.06.023.
Scott, E.R.D., Krot, A.N., 2014. Chondrites and their Components. In: Holland, H.D., Turekian, K.K. (Eds.), Treatise on Geochemistry, 2nd ed. Elsevier, Oxford, pp. 65–137. volume 1, doi: 10.1016/B978-0-08-095975-7.00104-2.
Shearer, C.K., Burger, P.V., Sutton, S.R., Papike, J.J., McCubbin, F., 2011. REE crystal chemistry of phosphates in extraterrestrial basalts at different oxygen fugacities: Direct determination of europium valence state in merrillite-whitlockite. Lunar Planet. Sci. Conf. 1143.
Shibazaki, Y., Ohtani, E., Terasaki, H., Suzuki, A., Funakoshi, K.i., 2009. Hydrogen partitioning between iron and ringwoodite: Implications for water transport into the Martian core. Earth Planet. Sci. Lett. 287, 463–470. https://doi.org/10.1016/j.epsl.2009.08.034.
Shukolyukov, A., Lugmair, G.W., 2006. Manganese-chromium isotope systematics of carbonaceous chondrites. Earth Planet. Sci. Lett. 250, 200–213. https://doi.org/10.1016/j.epsl.2006.07.036.
Siebert, J., Sossi, P.A., Blanchard, I., Mahan, B., Badro, J., Moynier, F., 2018. Chondritic Mn/Na ratio and limited post-nebular volatile loss of the Earth. Earth Planet. Sci. Lett. 485, 130–139. https://doi.org/10.1016/j.epsl.2017.12.042.
Simon, J.I., Jordan, M.K., Tappa, M.J., Schauble, E.A., Kohl, I.E., Young, E.D., 2017. Calcium and titanium isotope fractionation in refractory inclusions: tracers of condensation and inheritance in the early solar protoplanetary disk. Earth Planet. Sci. Lett. 472, 277–288. https://doi.org/10.1016/j.epsl.2017.05.002.
Smrekar, S.E., Lognonné, P., Spohn, T., Banerdt, W.B., Breuer, D., Christensen, U., Dehant, V., Drilleau, M., Folkner, W., Fuji, N., Garcia, R.F., Giardini, D., Golombek, M., Grott, M., Gudkova, T., Johnson, C., Khan, A., Langlais, B., Mittelholz, A., Mocquet, A., Myhill, R., Panning, M., Perrin, C., Pike, T., Plesa, A.C., Rivoldini, A., Samuel, H., Stähler, S.C., van Driel, M., Van Hoolst, T., Verhoeven, O., Weber, R., Wieczorek, M., 2019. Pre-mission InSights on the interior of Mars. Space Sci. Rev. 215, 3. https://doi.org/10.1007/s11214-018-0563-9.
Sossi, P.A., Klemme, S., O'Neill, H.S.C., Berndt, J., Moynier, F., 2019. Evaporation of moderately volatile elements from silicate melts: Experiments and theory. Geochim. Cosmochim. Acta 260, 204–231. https://doi.org/10.1016/j.gca.2019.06.021.
Sossi, P.A., Nebel, O., Anand, M., Poitrasson, F., 2016. On the iron isotope composition of Mars and volatile depletion in the terrestrial planets. Earth Planet. Sci. Lett. 449, 360–371. https://doi.org/10.1016/j.epsl.2016.05.030.
Sossi, P.A., Nebel, O., O'Neill, H.S.C., Moynier, F., 2018. Zinc isotope composition of the Earth and its behaviour during planetary accretion. Chem. Geol. 477, 73–84. https://doi.org/10.1016/j.chemgeo.2017.12.006.
Steenstra, E.S., Rai, N., Knibbe, J.S., Lin, Y.H., van Westrenen, W., 2016. New geochemical models of core formation in the Moon from metal-silicate partitioning of 15 siderophile elements. Earth Planet. Sci. Lett. 441, 1–9. https://doi.org/10.1016/j.epsl.2016.02.028.
Stolper, E., Paque, J.M., 1986. Crystallization sequences of Ca-Al-rich inclusions from Allende: The effects of cooling rate and maximum temperature. Geochim. Cosmochim. Acta 50, 1785–1806. https://doi.org/10.1016/0016-7037(86)90139-0.
Stracke, A., Palme, H., Gellissen, M., Münker, C., Kleine, T., Birbaum, K., Günther, D., Bourdon, B., Zipfel, J., 2012. Refractory element fractionation in the Allende

meteorite: Implications for solar nebula condensation and the chondritic composition of planetary bodies. Geochim. Cosmochim. Acta 85, 114–141. https://doi.org/10.1016/j.gca.2012.02.006.
Suer, T.A., Siebert, J., Remusat, L., Menguy, N., Fiquet, G., 2017. A sulfur-poor terrestrial core inferred from metal-silicate partitioning experiments. Earth Planet. Sci. Lett. 469, 84–97. https://doi.org/10.1016/j.epsl.2017.04.016.
Sugiura, N., Fujiya, W., 2014. Correlated accretion ages and ε^{54}Cr of meteorite parent bodies and the evolution of the solar nebula. Meteor. Planet. Sci. 49, 772–787. https://doi.org/10.1111/maps.12292.
Surkov, Y.A., Kirnozov, F.F., Glazov, V.N., Dunchenko, A.G., Tatsy, L.P., Sobornov, O.P., 1987. Uranium, thorium, and potassium in the Venusian rocks at the landing sites of Vega 1 and 2. J. Geophys. Res.: Solid Earth 92, E537–E540. https://doi.org/10.1029/JB092iB04p0E537.
Tait, K.T., Day, J.M.D., 2018. Chondritic late accretion to Mars and the nature of shergottite reservoirs. Earth Planet. Sci. Lett. 494, 99–108. https://doi.org/10.1016/j.epsl.2018.04.040.
Taylor, G.J., 2013. The bulk composition of Mars. Chemie der Erde-Geochemistry 73, 401–420. https://doi.org/10.1016/j.chemer.2013.09.006.
Taylor, G.J., Boynton, W., Brückner, J., Wänke, H., Dreibus, G., Kerry, K., Keller, J., Reedy, R., Evans, L., Starr, R., Squyres, S., Karunatillake, S., Gasnault, O., Maurice, S., d'Uston, C., Englert, P., Dohm, J., Baker, V., Hamara, D., Janes, D., Sprague, A., Kim, K., Drake, D., 2006. Bulk composition and early differentiation of Mars. J. Geophys. Res.: Planets 111, E03S10. https://doi.org/10.1029/2005JE002645.
Taylor, S.R., McLennan, S., 2009. Planetary Crusts: Their Composition, Origin and Evolution. volume 10. Cambridge University Press, Cambridge. https://doi.org/10.1017/CBO9780511575358.
Tenner, T.J., Ushikubo, T., Nakashima, D., Schrader, D.L., Weisberg, M.K., Kimura, M., Kita, N.T., 2018. Oxygen isotope characteristics of chondrules from recent studies by secondary ion mass spectrometry. In: Russell, S.S., Connolly, H.C.JJr., Krot, A.N. (Eds.), Chondrules: Records of Protoplanetary Disk Processes. Cambridge University Press, pp. 196–246. Cambridge Planetary Science. chapter 8, doi: 10.1017/9781108284073.008.
Tian, Z., Chen, H., Fegley Jr., B., Lodders, K., Barrat, J.A., Day, J.M.D., Wang, K., 2019. Potassium isotopic compositions of howardite-eucrite-diogenite meteorites. Geochim. Cosmochim. Acta 266, 611–632. https://doi.org/10.1016/j.gca.2019.08.012.
Trinquier, A., Birck, J.L., Allegre, C.J., 2007. Widespread ^{54}Cr heterogeneity in the inner solar system. Astrophys. J. 655, 1179. https://doi.org/10.1086/510360.
Trinquier, A., Birck, J.L., Allègre, C.J., Göpel, C., Ulfbeck, D., 2008. ^{53}Mn-^{53}Cr systematics of the early Solar System revisited. Geochim. Cosmochim. Acta 72, 5146–5163. https://doi.org/10.1016/j.gca.2008.03.023.
Trinquier, A., Elliott, T., Ulfbeck, D., Coath, C., Krot, A.N., Bizzarro, M., 2009. Origin of nucleosynthetic isotope heterogeneity in the solar protoplanetary disk. Science 324, 374–376. https://doi.org/10.1126/science.1168221.
Tsuno, K., Grewal, D.S., Dasgupta, R., 2018. Core-mantle fractionation of carbon in Earth and Mars: The effects of sulfur. Geochim. Cosmochim. Acta 238, 477–495. https://doi.org/10.1016/j.gca.2018.07.010.
Turcotte, D., Schubert, G., 2014. Geodynamics, 3rd ed. Cambridge University Press, Cambridge. https://doi.org/10.1017/cbo9780511843877.
Turcotte, D.L., Paul, D., White, W.M., 2001. Thorium-uranium systematics require layered mantle convection. J. Geophys. Res.: Solid Earth 106, 4265–4276. https://doi.org/10.1029/2000JB900409.
Urey, H.C., Craig, H., 1953. The composition of the stone meteorites and the origin of the meteorites. Geochim. Cosmochim. Acta 4, 36–82. https://doi.org/10.1016/0016-7037(53)90064-7.
Villeneuve, J., Chaussidon, M., Libourel, G., 2009. Homogeneous distribution of ^{26}Al in the solar system from the Mg isotopic composition of chondrules. Science 325, 985–988. https://doi.org/10.1126/science.1173907.
Wade, J., Wood, B.J., Tuff, J., 2012. Metal-silicate partitioning of Mo and W at high pressures and temperatures: evidence for late accretion of sulphur to the Earth. Geochim. Cosmochim. Acta 85, 58–74. https://doi.org/10.1016/j.gca.2012.01.010.
Wadhwa, M., 2001. Redox state of Mars' upper mantle and crust from Eu anomalies in shergottite pyroxenes. Science 291, 1527–1530. https://doi.org/10.1126/science.1057594.
Wadhwa, M., 2008. Redox conditions on small bodies, the Moon and Mars. In: MacPherson, G.J. (Ed.), Rev. Mineral. Geochem. Mineralogical Society of America, pp. 493–510 volume 68, doi: 10.2138/rmg.2008.68.17.
Walker, R.J., Bermingham, K., Liu, J., Puchtel, I.S., Touboul, M., Worsham, E.A., 2015. In search of late-stage planetary building blocks. Chem. Geol. 411, 125–142. https://doi.org/10.1016/j.chemgeo.2015.06.028.
Walsh, K.J., Morbidelli, A., Raymond, S.N., O'Brien, D.P., Mandell, A.M., 2011. A low mass for Mars from Jupiter's early gas-driven migration. Nature 475, 206–209. https://doi.org/10.1038/nature10201.
Wang, H., Weiss, B.P., Bai, X.N., Downey, B.G., Wang, J., Wang, J., Suavet, C., Fu, R.R., Zucolotto, M.E., 2017. Lifetime of the solar nebula constrained by meteorite paleomagnetism. Science 355, 623–627. https://doi.org/10.1126/science.aaf5043.
Wang, Z., Becker, H., 2017. Chalcophile elements in Martian meteorites indicate low sulfur content in the Martian interior and a volatile element-depleted late veneer. Earth Planet. Sci. Lett. 463, 56–68. https://doi.org/10.1016/j.epsl.2017.01.023.
Wänke, H., 1981. Constitution of terrestrial planets. Philos. Trans. Royal Soc. London. Series A: Math. Phys. Sci. 303, 287–302. https://doi.org/10.1098/rsta.1981.0203.
Wänke, H., Dreibus, G., 1988. Chemical composition and accretion history of terrestrial planets. Philos. Trans. Royal Soc. London. Series A: Math. Phys. Sci. 325, 545–557. https://doi.org/10.1098/rsta.1988.0067.
Wänke, H., Dreibus, G., 1994. Chemistry and accretion history of Mars. Philos. Trans. Royal Soc. London. Series A: Math. Phys. Sci. 349, 285–293. https://doi.org/10.1098/rsta.1994.0132.
Wänke, H., Dreibus, G., Jagoutz, E., 1984. Mantle chemistry and accretion history of the Earth. In: Kröner, A., Hanson, G.N., Goodwin, A.M. (Eds.), Archaean Geochemistry. Springer, pp. 1–24. https://doi.org/10.1007/978-3-642-70001-9_1.
Warren, P.H., 2005. "New" lunar meteorites: Implications for composition of the global lunar surface, lunar crust, and the bulk Moon. Meteor. Planet. Sci. 40, 477–506. https://doi.org/10.1111/j. 1945-5100.2005.tb00395.x.
Warren, P.H., 2008. A depleted, not ideally chondritic bulk Earth: The explosive-volcanic basalt loss hypothesis. Geochim. Cosmochim. Acta 72, 2217–2235. https://doi.org/10.1016/j.gca.2007.11.038.
Warren, P.H., 2011. Stable-isotopic anomalies and the accretionary assemblage of the Earth and Mars: A subordinate role for carbonaceous chondrites. Earth Planet. Sci. Lett. 311, 93–100. https://doi.org/10.1016/j.epsl.2011.08.047.
Wasserburg, G.J., MacDonald, G.J.F., Hoyle, F., Fowler, W.A., 1964. Relative contributions of uranium, thorium, and potassium to heat production in the Earth. Science 143, 465–467. https://doi.org/10.1126/science.143.3605.465.
Wasserburg, G.J., Mazor, E., Zartman, R.E., 1963. Isotopic and chemical composition of some terrestrial natural gases. In: Geiss, J., Goldberg, E.D. (Eds.), Earth Science and Meteorites. North-Holland Pub. Co, pp. 219–240.
Wasson, J.T., Kallemeyn, G.W., 1988. Compositions of chondrites. Philos. Trans. Royal Soc. London A: Math. Phys. Eng. Sci. 325, 535–544. https://doi.org/10.1098/rsta.1988.0066.
Wasson, J.T., Krot, A.N., Lee, M.S., Rubin, A.E., 1995. Compound chondrules. Geochim. Cosmochim. Acta 59, 1847–1869. https://doi.org/10.1016/0016-7037(95)00087-G.
Wasson, J.T., Richardson, J.W., 2001. Fractionation trends among IVA iron meteorites: Contrasts with IIIAB trends. Geochim. Cosmochim. Acta 65, 951–970. https://doi.org/10.1016/S0016-7037(00)00597-4.
Weisberg, M.K., Ebel, D.S., Connolly, H.C., Kita, N.T., Ushikubo, T., 2011. Petrology and oxygen isotope compositions of chondrules in E3 chondrites. Geochim. Cosmochim. Acta 75, 6556–6569. https://doi.org/10.1016/j.gca.2011.08.040.
Wheeler, K.T., Walker, D., McDonough, W.F., 2011. Pd and Ag metal-silicate partitioning applied to Earth differentiation and core-mantle exchange. Meteor. Planet. Sci. 46, 199–217. https://doi.org/10.1111/j.1945-5100.2010.01145.x.
Wiechert, U., Halliday, A.N., 2007. Non-chondritic magnesium and the origins of the inner terrestrial planets. Earth Planet. Sci. Lett. 256, 360–371. https://doi.org/10.1016/j.epsl.2007.01.007.
Wiechert, U., Halliday, A.N., Lee, D.C., Snyder, G.A., Taylor, L.A., Rumble, D., 2001. Oxygen isotopes and the Moon-forming giant impact. Science 294, 345–348. https://doi.org/10.1126/science.1063037.
Wieczorek, M.A., Zuber, M.T., 2004. Thickness of the Martian crust: Improved constraints from geoid-to-topography ratios. J. Geophys. Res.: Planets 109. https://doi.org/10.1029/2003JE002153.
Willig, M., Stracke, A., Beier, C., Salters, V.J.M., 2020. Constraints on mantle evolution from Ce-Nd-Hf isotope systematics. Geochim. Cosmochim. Acta 272, 36–53. https://doi.org/10.1016/j.gca.2019.12.029.
Wipperfurth, S.A., Guo, M., Šrámek, O., McDonough, W.F., 2018. Earth's chondritic Th/U: Negligible fractionation during accretion, core formation, and crust-mantle differentiation. Earth Planet. Sci. Lett. 498, 196–202. https://doi.org/10.1016/j.epsl.2018.06.029.
Wipperfurth, S.A., Šrámek, O., McDonough, W.F., 2020. Reference models for lithospheric geoneutrino signal. J. Geophys. Res.: Solid Earth 125 e2019JB018433, doi: 10.1029/2019JB018433.
Wombacher, F., Rehkämper, M., Mezger, K., Bischoff, A., Münker, C., 2008. Cadmium stable isotope cosmochemistry. Geochim. Cosmochim. Acta 72, 646–667. https://doi.org/10.1016/j.gca.2007.10.024.
Wood, B.J., Smythe, D.J., Harrison, T., 2019. The condensation temperatures of the elements: A reappraisal. Am. Mineral. 104, 844–856. https://doi.org/10.2138/am-2019-6852CCBY.
Wood, B.J., Wade, J., Kilburn, M.R., 2009. Core formation and the oxidation state of the Earth: Additional constraints from Nb, V and Cr partitioning. Geochim. Cosmochim. Acta 72, 1415–1426. https://doi.org/10.1016/j.gca.2007.11.036.
Yang, S., Humayun, M., Righter, K., Jefferson, G., Fields, D., Irving, A.J., 2015. Siderophile and chalcophile element abundances in shergottites: Implications for Martian core formation. Meteor. Planet. Sci. 50, 691–714. https://doi.org/10.1111/maps.12384.
Yoder, C.F., Konopliv, A.S., Yuan, D.N., Standish, E.M., Folkner, W.M., 2003. Fluid core size of Mars from detection of the solar tide. Science 300, 299–303. https://doi.org/10.1126/science.1079645.
Yoshizaki, T., McDonough, W.F., 2020. The composition of Mars. Geochim. Cosmochim. Acta 273, 137–162. https://doi.org/10.1016/j.gca.2020.01.011.
Yoshizaki, T., Nakashima, D., Nakamura, T., Park, C., Sakamoto, N., Ishida, H., Itoh, S., 2019. Nebular history of an ultrarefractory phase bearing CAI from a reduced type CV chondrite. Geochim. Cosmochim. Acta 252, 39–60. https://doi.org/10.1016/j.gca.2019.02.034.
Young, E.D., Galy, A., 2004. The isotope geochemistry and cosmochemistry of magnesium. Rev. Mineral. Geochem. 55, 197–230. https://doi.org/10.2138/gsrmg.55.1.197.
Young, E.D., Kohl, I.E., Warren, P.H., Rubie, D.C., Jacobson, S.A., Morbidelli, A., 2016. Oxygen isotopic evidence for vigorous mixing during the Moon-forming giant impact. Science 351, 493–496. https://doi.org/10.1126/science.aad0525.
Young, E.D., Shahar, A., Nimmo, F., Schlichting, H.E., Schauble, E.A., Tang, H., Labidi, J., 2019. Near-equilibrium isotope fractionation during planetesimal evaporation. Icarus 323, 1–15. https://doi.org/10.1016/j.icarus.2019.01.012.

Zanda, B., Lewin, É., Humayun, M., 2018. The chondritic assemblage. In: Russell, S.S., Connolly, H.C.JJr., Krot, A.N. (Eds.), Chondrules: Records of Protoplanetary Disk Processes. Cambridge University Press, Cambridge, pp. 122–150 volume 22. chapter 5, doi: 10.1017/9781108284073.005.

Zhang, J., Dauphas, N., Davis, A.M., Leya, I., Fedkin, A., 2012. The proto-Earth as a significant source of lunar material. Nature Geoscience 5, 251–255. https://doi.org/10.1038/ngeo1429.

Zhu, K., Moynier, F., Schiller, M., Bizzarro, M., 2020. Dating and tracing the origin of enstatite chondrite chondrules with Cr isotopes. Astrophys. J. Lett. 894, L26. https://doi.org/10.3847/2041-8213/ab8dca.

Zuber, M.T., Solomon, S.C., Phillips, R.J., Smith, D.E., Tyler, G.L., Aharonson, O., Balmino, G., Banerdt, W.B., Head, J.W., Johnson, C.L., Lemoine, F.G., McGovern, P. J., Neumann, G.A., Rowlands, D.D., Zhong, S., 2000. Internal structure and early thermal evolution of Mars from Mars Global Surveyor topography and gravity. Science 287, 1788–1793. https://doi.org/10.1126/science.287.5459.1788.